

International Atomic Energy Agency

IN DC

INTERNATIONAL NUCLEAR DATA COMMITTEE

Central Scientific Research Institute for Information
and Technico-Economic Investigation in Nuclear
Science and Technology

Questions of Nuclear Science and Technology

NUCLEAR CONSTANTS

Issue No. 12
(Part II)

RESULTS OBTAINED IN STUDIES ON PHOTONEUTRON
REACTIONS NEAR THE THRESHOLD

A.I. Abramov

Vienna, June 1975

IAEA NUCLEAR DATA SECTION, KÄRNTNER RING 11, A-1010 VIENNA

75-3197

Translated from Russian

Central Scientific Research Institute for Information
and Technico-Economic Investigation in Nuclear
Science and Technology

QUESTIONS OF NUCLEAR SCIENCE AND TECHNOLOGY

Nuclear Constants
Issue 12
(Part II)

RESULTS OBTAINED IN STUDIES ON PHOTONEUTRON
REACTIONS NEAR THE THRESHOLD

A.I. Abramov

Moscow - 1974

UDK 539.17(048) + 539.173.3(048) + 539.173.84(048)

This issue is a compilation of the main information obtained during recent years (1966-72) in studies on photoneutron reactions near the threshold. Data are given in various forms: graphs of the energy dependence of differential cross-sections for (γ ,n) reactions, parameters of observed resonances (E^{lab} , Γ_{γ_0} , g_{γ} , Γ_n , J^A , etc.), evaluations of radiation strength functions $S_{\gamma_0} = \langle \Gamma_{\gamma_0} / D \rangle$, of non-resonance cross-sections and of other doorway state phenomena. Presented in the form of a reference book, the data should prove useful to a wide range of specialists studying the properties of atomic nuclei.

Editors

V.A. Kuznetsov (Senior Scientific Editor), L.N. Usachev (Deputy Senior Scientific Editor), O.D. Kazachkovskij, S.M. Feinberg, V.G. Zagrafov, V.V. Orlov, P.E. Nemirovskij, V.I. Mostovoj, V.G. Zolotukhin, S.I. Sukhoruchkin, M.N. Nikolayev, E.I. Lyashenko, B.G. Dubovskij, A.A. Abagyan, I.G. Morozov, D.A. Kardashev (Chief Editor).

FOREWORD

This compilation presents the main results of studies on photoneutron reactions near the threshold, taken from work published before 1 January 1973. Wherever a particular group of authors published several studies in the same connection, only the results of their most recent work are given. In order to speed up release of the information and to enhance its transmission reliability, all the graphs are presented in the form of photocopies of the source material.

The elements for which data are given are arranged in order of their numbers in the periodic table, and for each individual element the data are given in the numerical order of the mass numbers of the isotopes. In the top right-hand corner of each page we give the periodic table number, the symbol for the element and the mass number. Where the data relate to a natural mixture of isotopes, this is indicated by the letters "nat" instead of the mass number; data of this kind come before the data for the individual isotopes.

The data given for each element are broken down as follows:

Isotopic content (precedes the data for natural mixtures of isotopes).

Information is given on the abundance of the various isotopes $p(\%)$ and their neutron binding energy Q_n (MeV).

Level scheme (Precedes the data for individual isotopes). In the centre of the scheme are given the values of p and J^π for the ground state of the parent nucleus together with the spin characteristics of levels which can be excited in EI and MI transitions. On the left is shown the arrangement of lower levels of the residual nucleus $A-1$ with their spin characteristics and excitation energy in keV. On the right-hand side, the energy scale is given in the centre-of-mass system (CMS): the first figure shown above 0 is the neutron binding energy in the parent nucleus Q_n (MeV), which is also the reaction threshold energy in the CMS. The values Q_n are taken from tables of Kravtsov[2d] and [17d] Gove and Wapstra. The figures given higher up the axis are the sums of Q_n and the excitation energies for the corresponding levels of the residual nucleus, which in the CMS are the threshold energies of (γ, n) reactions with formation of a residual nucleus in some excited state: $E_c^{\text{th}} = Q_n + E_c^{\text{lev}}$. To a first approximation the values of E_c^{th} indicate the minimum values of bremsstrahlung end-point energy E_γ^{max} for which

these processes are possible. More exact values of threshold energy E_c^{th} in the laboratory system of co-ordinates can be obtained from the E_c^{th} values using the well-known formula

$$E^{th} \approx E_c^{th} \left(1 + \frac{E_c^{th}}{2 M c^2} \right)$$

where M is the mass of the parent nucleus.

The differential cross-sections are presented in graphical form only. The main details of the experimental conditions are given under the diagram: the maximum bremsstrahlung energy E_γ^{max} (or accelerated electron energy E_e), the angle ϑ between electron beam axis and direction from sample to neutron detector, energy resolution of the spectrometer, type and composition of the test sample, etc.

Photoneutron yield. Data given under this heading have been presented by their authors in "rough" form: the number of counts per analyser channel as a function of channel number. This type of information is given either when differential cross-section data for the type of nucleus under consideration are lacking or when they differ from the results given. For the rest, the arrangement of the material is similar to that under the heading "Differential cross-sections".

Resonance parameters. The following data are given in tabular form: neutron energies E_n^{lab} , in the laboratory system of co-ordinates, corresponding to the maximum observed resonance peaks, partial widths of radiative transitions to the ground state of the parent nucleus $\Gamma_{\gamma 0}$, combinations of these widths with other widths and with the spin factor g_γ , values of J^π . The symbols GS and ES denote transitions to the ground and excited states of the residual nucleus, respectively. The last column gives the neutron energies E_n^{res} at which the corresponding resonances are observed in neutron experiments (total cross-section measurements, scattering cross-section measurements, etc.). The values of E_n^{res} taken from studies on gamma rays (e.g. Baglan, et al.[27]) were obtained by converting the measured values of E_n^{lab} using well-known formulae.

For some of the isotopes in the tables data are given from various works for comparison. In such cases, when the values of E_n^{lab} are similar and it can be assumed that the data given refer to the same resonance, all

the details are written in one line; when this procedure is unclear, the data are written in different lines.

Radiation strength function $S_\gamma = \langle \Gamma_{\gamma_0} / D \rangle$. This physical quantity can be estimated whenever information is available on the values of Γ_{γ_0} and of the nuclear level density, but in this book only the values of S_{γ_0} obtained by the authors of original studies are given.

Non-resonance cross-sections σ_{NR} (cross-sections of a non-resonance process) are taken from evaluations in which the asymmetry found in the individual resonance peaks is attributed to interference of the amplitudes of direct and resonance mechanisms.

Doorway states. Consideration is given to the possibility of explaining some of the phenomena observed (level grouping, correlations between partial widths, etc.) by the production of so-called "doorway states"; the validity of such explanations is also assessed.

The Annexes contain a compilation of reference data which may prove useful for specialists studying photoneutron reactions near the threshold.

Annex 1 consists of a table giving the main characteristics of all stable and long-lived isotopes contained in a natural mixture: mass number, spin and parity, abundance, neutron binding energy Q_n , decay type and period of the residual nucleus formed by the (γ, n) reaction. In cases where the formation of long-lived isomers is possible, two half-lives are given separated by the sign (+); the symbol IT is used to designate isomeric transitions for nuclei which are stable in the ground state. The values of Q_n were taken from Kravtsov[2d] and Gove and Wapstra[17d], and the remaining data from Dzhelepov, Peker and Sergeev[1d].

Annex 2 is a bibliographic index of studies on photoneutron reactions near the threshold, as of 1 January 1973. Its structure is based on the well-known CINDA system, which has been successfully used for a number of years, on an international scale, for indexing neutron data. Slight modifications of this system, allowing it to be used to describe a wider class of reactions, are described by Abramov[18d]. The tables in Annex 2 are print-outs of M-222 computer punched cards. Transferring the index to computer carriers required certain changes in the entry, compared with Abramov's study[18d], namely:

(1) The length of the line is shortened from 128 to 120 characters by reducing the spacing between the columns to one character (except for the space preceding the "Comments"). This was necessary so that all the information recorded in one line could be fitted on to a single M-222 punched card;

(2) Changes in column headings:

DATA TYPE - type of data presented;

E PRIM - energy of primary particles (gamma quanta);

E SEC - energy of secondary particles (neutrons);

NT - Nature of the work (experimental, theoretical, etc.) and

Type of publication (article in journal, report, etc.);

YEAR - date work was published (month and year);

(3) For the sake of standardization the symbols for certain quantities were changed:

Before

ANALG STATES

NON RESN GN

In this work

ANALG STS

GN NON RESN

(4) A separating sign (;) was introduced in the "Comments", and the abbreviation IPI (= J^K) was added to the thesaurus of measured quantities.

The primary sources used in the work are given in two lists.

The first (main) list contains papers devoted to the study of photoneutron reactions near the threshold. Figures in square brackets (e.g. [27]) are references in this list.

The second (supplementary) list contains studies, findings of which are used in analysing the main data (level-scheme data, neutron binding energies in nuclei etc.). Figures followed by the letter "d" in square brackets (e.g. [9d]) are references in this list.

BERYLLIUM-9

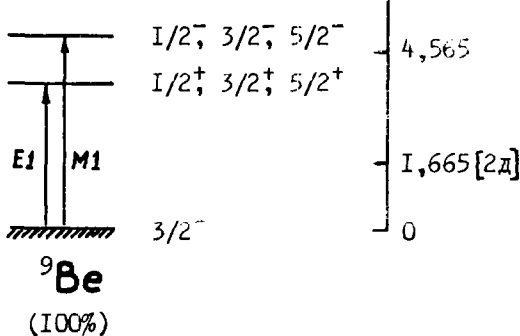
4 - Be - 009

Level scheme [1d]

2^+ 2900 —

0^+ 0 —

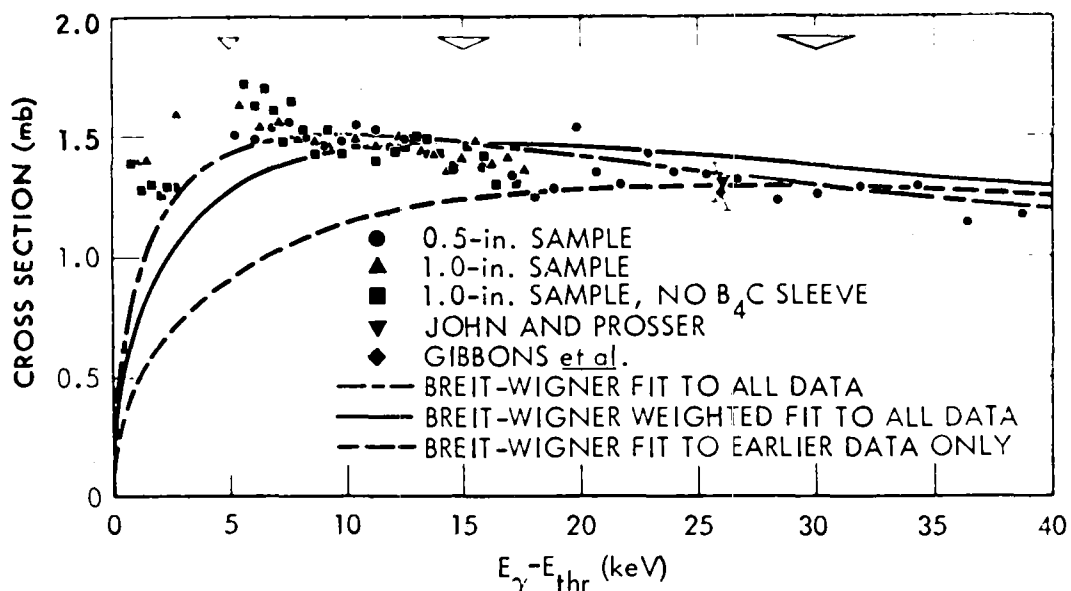
$^{8\text{Be}}$



$^{9\text{Be}}$

(100%)

Effective cross-sections of (γ ,n) reactions [5]



$$E_{\gamma}^{\max} = 3.5 \text{ MeV}$$

$$\theta = 135^\circ$$

The quantity $E_{\gamma} - E_{\text{thr}}^{\text{th}}$ is plotted along the axis of abscissa and, within the accuracy of the kinematic corrections, it is equal to E_n^{lab} .

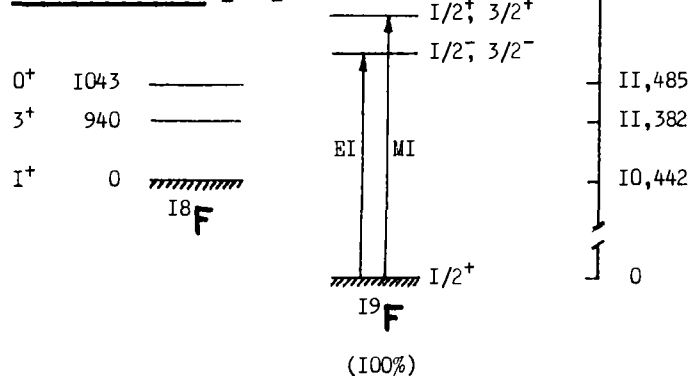
The graph shows total cross-sections of (γ ,n) reactions, obtained from differential cross-sections by multiplying by 4π , and normalized to the results of Refs [3d] ♦ and [4d] ▼ for $E_{\gamma} - E_{\text{thr}}^{\text{th}} = 26 \text{ keV}$.

The energy resolution is 30 nsec/m; corresponding values of ΔE are shown by the triangles in the upper part of the figure.

FLUORINE-19

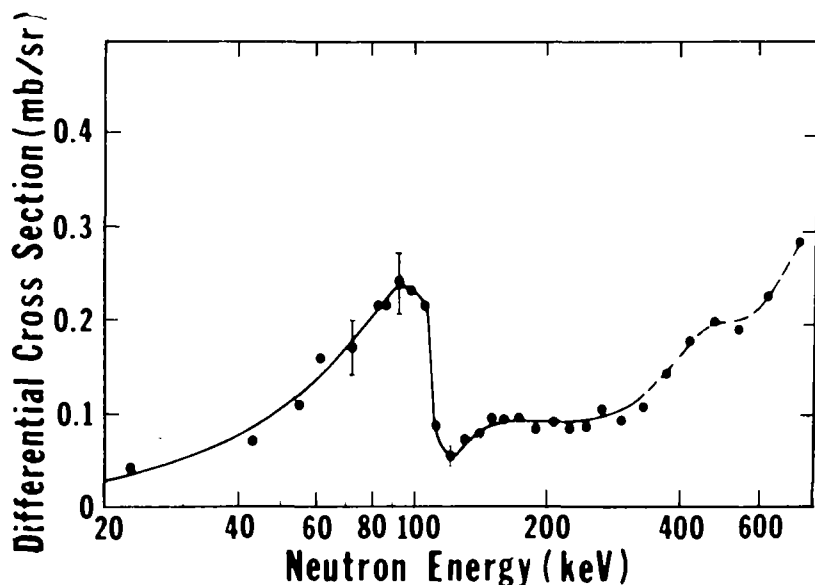
9 - F - 019

Level scheme [1d]



(100%)

Differential cross-sections [27]



$$\begin{aligned} E_{\gamma}^{\max} &= 11.7 \text{ MeV} \\ \theta &= 135^\circ \end{aligned}$$

Resolution = 3.5 nsec/m

Resonance parameters [27]

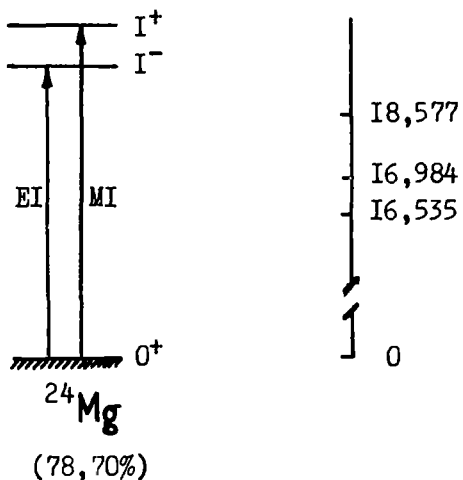
E_n^{lab} (keV)	$g \Gamma_{\gamma 0} \Gamma_n / \Gamma$	GS or ES
100	1.8	GS

MAGNESIUM-24

I₂ - Mg - 024

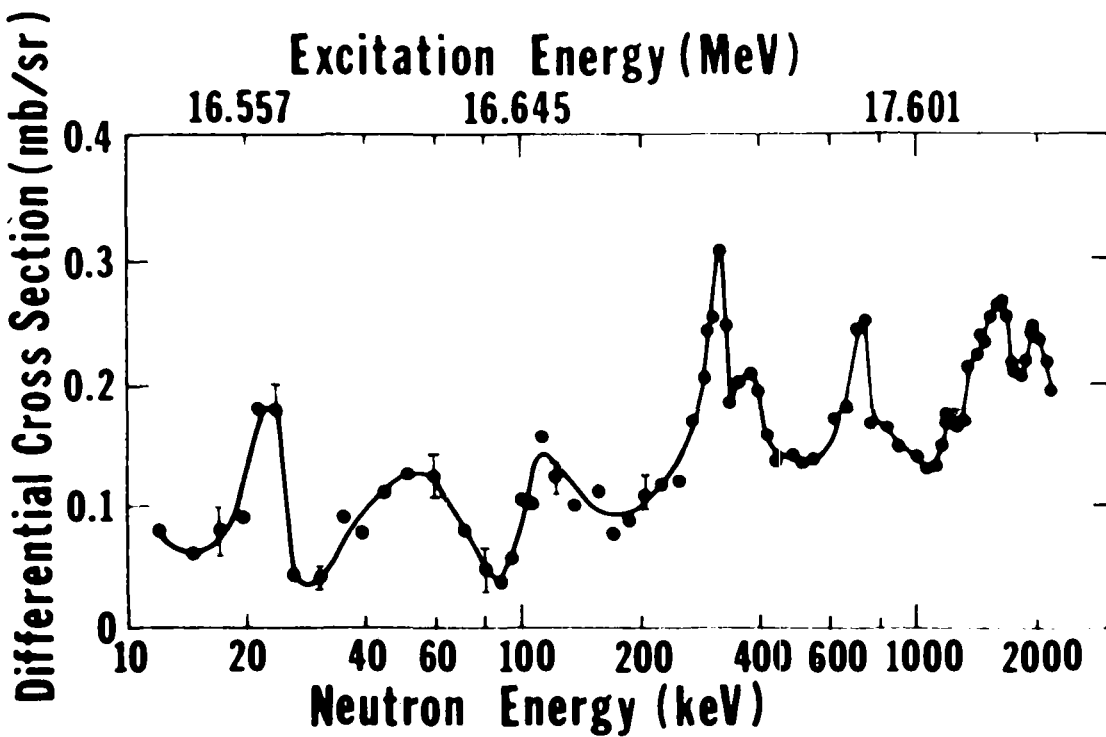
Level scheme [1d]

2042 —
5/2⁺ 449 —
3/2⁺ 0
²³Mg



(78, 70%)

Differential cross-sections [27]



$$E_{\gamma}^{\max} = 19.5 \text{ MeV}$$

$$\theta = 135^\circ$$

Resolution = 2.3 nsec/m

Sample - magnesium oxide. Isotopic composition: ²⁴Mg: ²⁵Mg: ²⁶Mg = 99.9:0.08:0.01. Weight of magnesium-24 - 113 g.

I₂ - Mg - 024

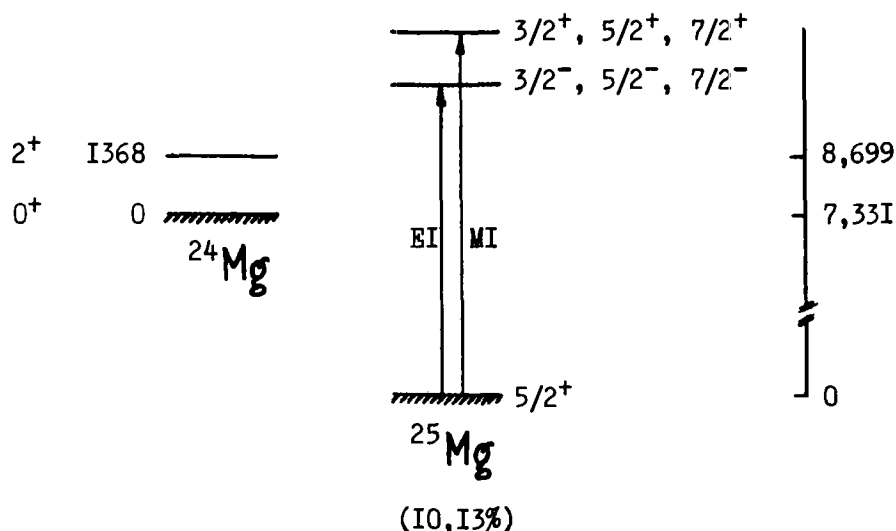
Resonance parameters [27]

E _n ^{lab} (keV)	g _r Γ _{γo} Γ _n /Γ (eV)	GS or ES	J ^π	Γ _{γo} (eV)
22	0,61		(I ⁻)	0,40
55	2,4	GS	(I ⁻)	1,6
110	4,0	GS	(I ⁻)	2,7
312	10,7		(I ⁻)	7,1
382				
717	19,5		(I ⁻)	13,0
1210				
1620				
1955				

MAGNESIUM-25

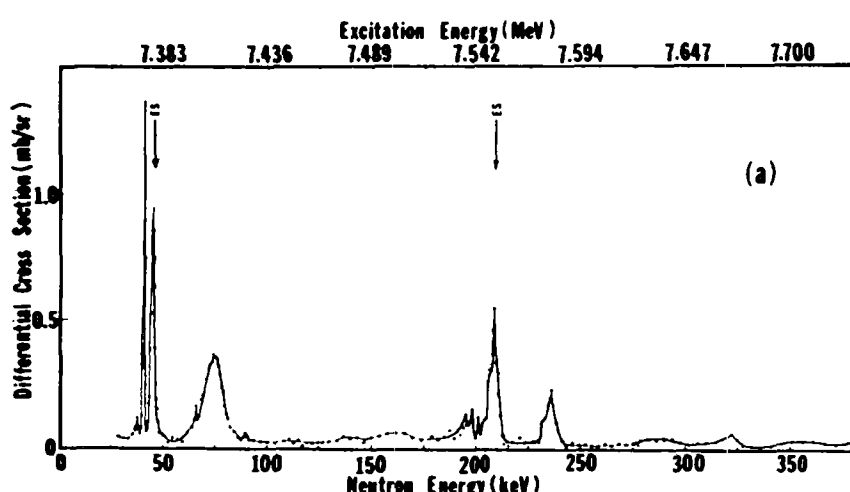
I2 - Mg - 025

Level scheme [1d]



(10, 13%)

Differential cross-sections [16, 27]



$$E_{\gamma}^{\max} = 11.0 \text{ MeV}$$

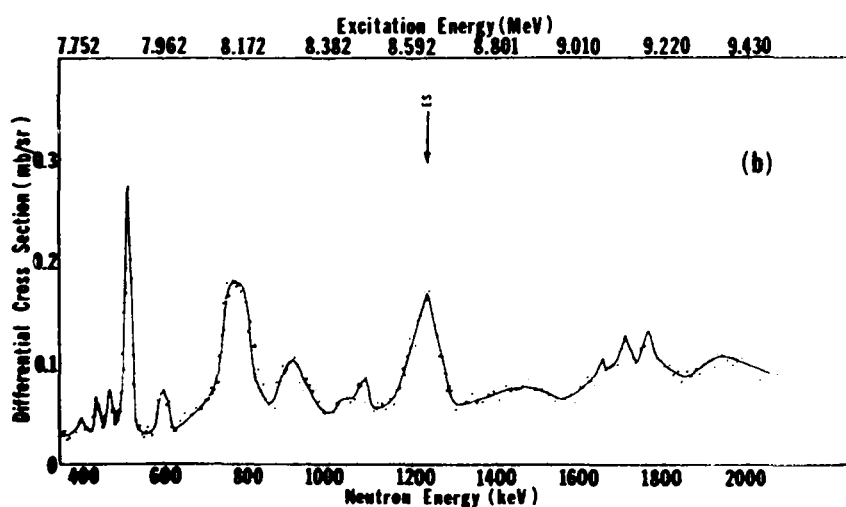
$$\theta = 135^\circ$$

Resolution = 1.6 nsec/m

Sample - magnesium oxide. Isotopic composition: $^{24}\text{Mg}:^{25}\text{Mg}:^{26}\text{Mg} = 1.86:97.87:0.26$. Weight of magnesium-25 - 29.7 g.

Arrows indicate peaks corresponding to transitions to excited levels of the residual magnesium-24 nucleus.

I2 - Mg - 025



See subscripts to Fig. (a). Range of higher neutron energies.

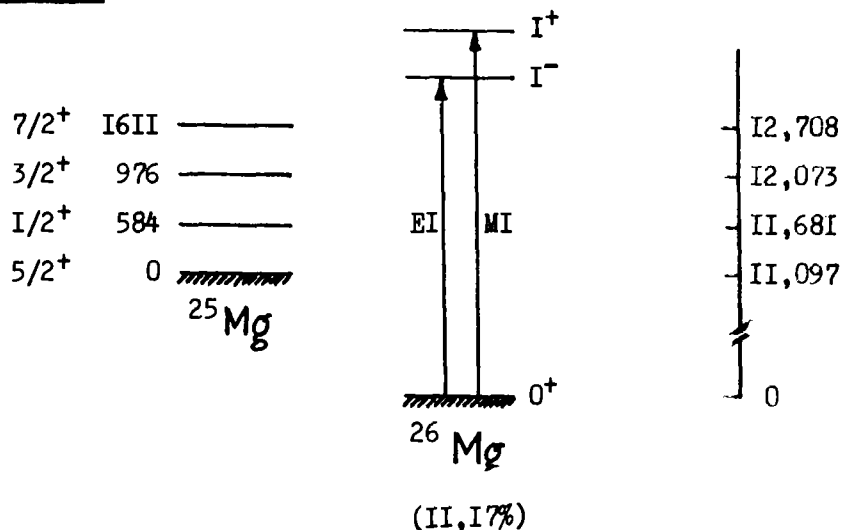
Resonance parameters [27]

E_n^{lab} (keV)	$g_{\gamma} \Gamma_{\gamma 0} / \Gamma$ (eV)	GS or ES	J^π	$\Gamma_{\gamma 0}$ (eV)	E_n^{res} (keV)
4I, I	0,09	GS			
45, I	0,3I	ES			
74, 9	0,36	GS	$3/2^-$	I, I	84, I
208	0,29	ES			
236	0,09	GS			26I
404	0,03				445
439	0,05		$5/2^+$		484
472	0,06				520
5I5	0,46	GS	$3/2^+$		567
60I	0,18				66I
78I	I, 5I				857
9I2	0,72				I003
I236	2,4	ES	$3/2^+, 5/2^+$		
I707					I869
I764					I93I

MAGNESIUM-26

I2 - Mg- 026

Level scheme [1d]



(II,I7%)

Resonance parameters [27]

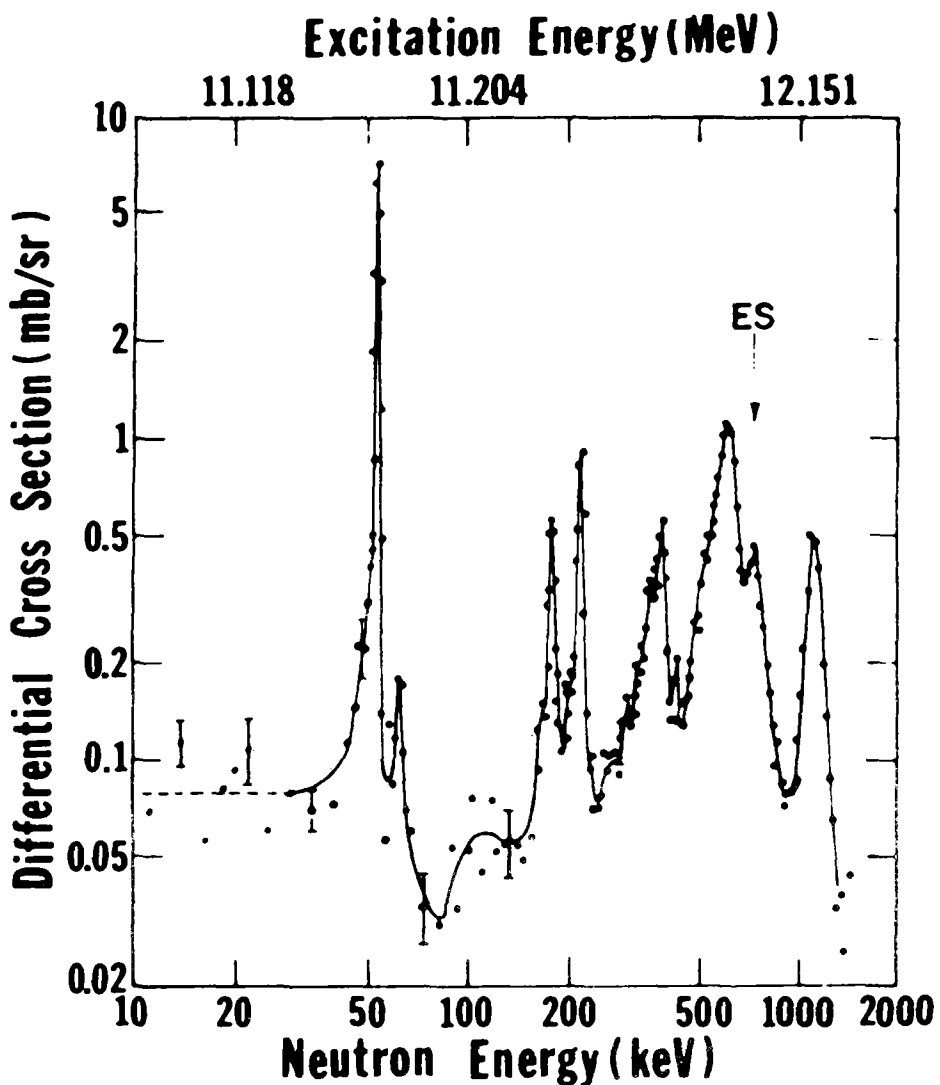
E_n^{lab} (keV)	$g_1 \Gamma_{\gamma} \cdot \Gamma_n / \Gamma$ (eV)	GS or ES	J^π	Γ_{γ} (eV)	E_n^{res} (keV)
54,3	2,6	GS	$I^-(I^+, 2^+)$	I,75	62,3
63,2	0,05			0,034	72,2
I8I	I,0	GS	$I^-(I^+, 2^+)$	0,68	202
222	I,9	GS	$I^-(I^+, 2^+)$	I,3	248
39I	5,I	GS	$I^-(I^+, 2^+)$	3,5	433
62I	32,5	GS	$I^-(I^+, 2^+)$	22,2	684
738	I5,0	ES		5,I	
II22	I4,7	GS	$I^-(I^+, 2^+)$	I0,0	I232

Radiation strength function [27]

$$\langle \Gamma_{\gamma} / D \rangle = (3,1 \pm 2,0) \cdot 10^{-5}$$

I₂ - Mg- 026

Differential cross-sections [10, 27]



$$E_n^{\max} = 13.3 \text{ MeV}$$

$$\theta = 135^\circ$$

Resolution - 2.3 nsec/m

Sample - magnesium oxide. Isotopic composition: $^{24}\text{Mg}:^{25}\text{Mg}:^{26}\text{Mg} = 0.21:0.09:99.7$.

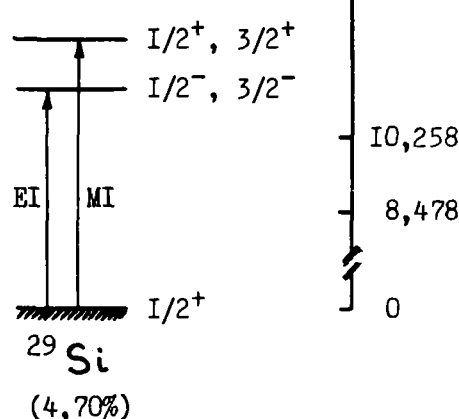
Arrow indicates a peak corresponding to the transition to an excited level of the residual magnesium-25 nucleus.

SILICON-29

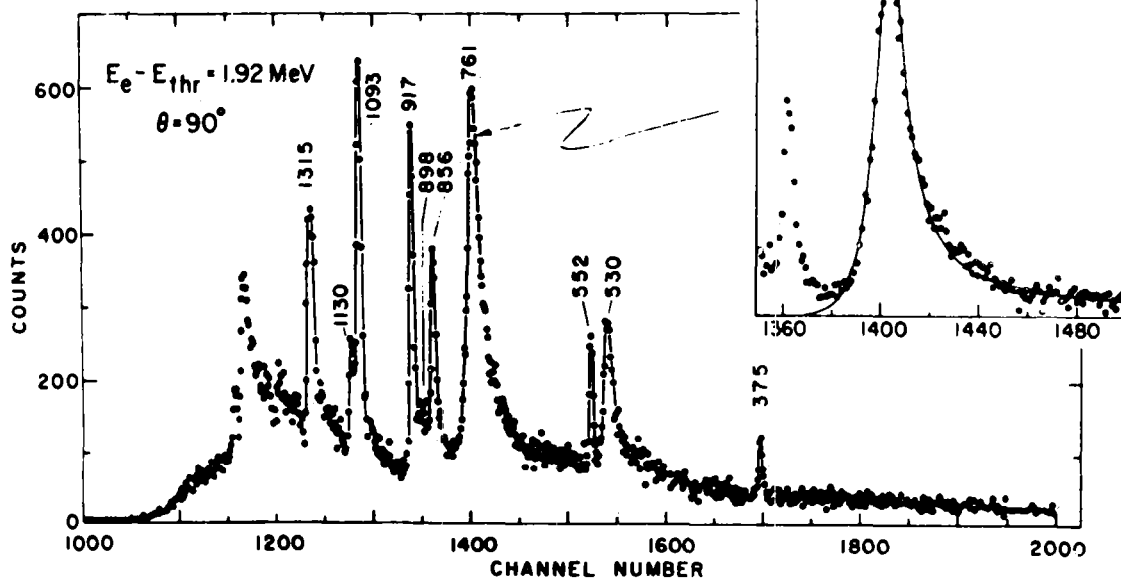
I4 - Si - 029

Level scheme [1d]

2^+ I780 —
 0^+ 0 
 ^{28}Si



Photoneutron yield [40]



$E_e - E_{thr} = 1.92 \text{ MeV}$ ($E_\gamma^{\max} = 10.4 \text{ MeV}$)
 $\theta = 90^\circ$

Sample - 63 g of SiO_2 enriched to ^{29}Si 95%.

No account is taken of variations in detector sensitivity with neutron energy or of the energy dependence of the gamma radiation flux.

Near the resonances the values of E_n^{lab} are given in keV.

Transitions are observed only to the ground state of the ^{28}Si nucleus.

The resonance with $E_n^{\text{lab}} = 761 \text{ keV}$ is shown expanded in the insert.
The continuous curve represents calculations based on the Breit-Wigner formalism with $\Gamma = 26 \text{ keV}$ and $a_{NR} = 0.32 \text{ mbarn}$.

Non-resonance cross-section [40]

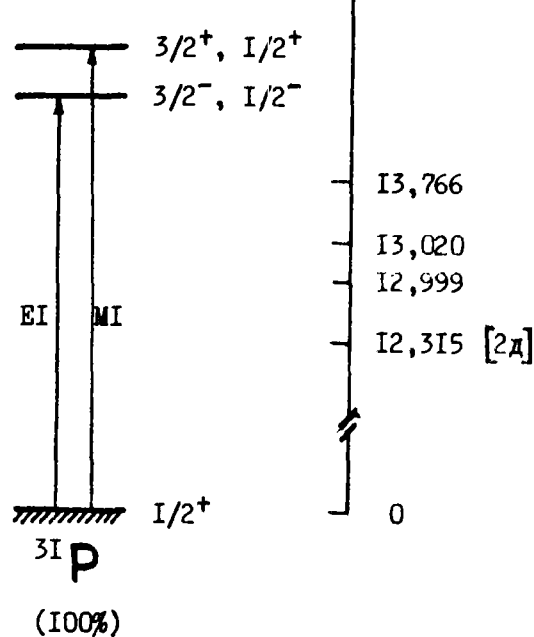
$$\sigma_{\text{NR}} = 0.32 \text{ mbarn}$$

PHOSPHORUS-31

IS - P - 03I

Level scheme [1d]

2^+ 1451 —
 1^+ 705 —
 0^+ 684 —
 I^+ 0 
 ^{30}P



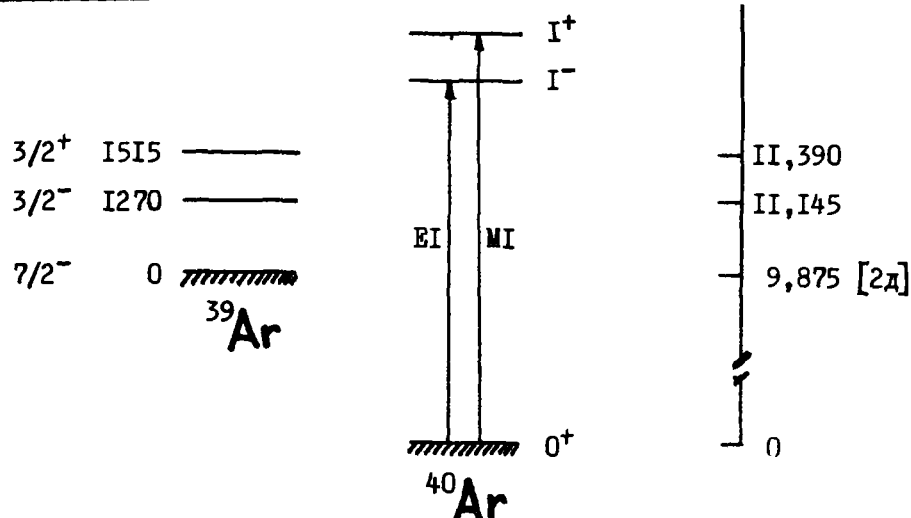
Resonance parameters [27]

E_n^{lab} (keV)	$g \Gamma_\gamma \Gamma_n / \Gamma$ (eV)
109	0,86
280	0,60
398	0,59
678	0,90
939	4,4

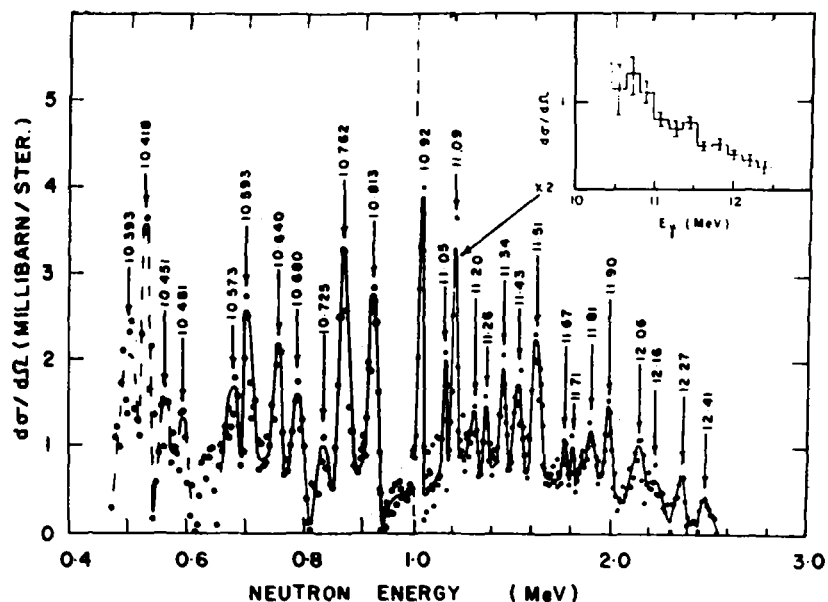
ARGON-40

I8 - Ar - 040

Level scheme [1d]



Differential cross-sections [39]



$$E_{\gamma}^{\max} = 12.6 \text{ MeV}$$

$$\theta = 90^\circ$$

Resolution = 0.6–0.9 nsec/m

The figures near the arrows represent the excitation energies of the ^{40}Ar nucleus.

All observed peaks correspond to the formation of a ^{39}Ar nucleus in the ground state.

Cross-sections averaged for intervals of $E = 200$ keV are shown in the insert.

I8 - Ar - 040

Resonance parameters [39]

Excitation energy (MeV)	$g \Gamma_{\rho^0}^*$ (eV)	$\Gamma_{\rho^0}^{**}$ (eV)
I0,393	(II,3)	(7,5)
I0,418	(9,6)	(6,4)
I0,451	(5,0)	(3,3)
I0,481	(5,0)	(3,4)
I0,573	7,3	4,9
I0,593	8,I	5,4
I0,640	9,3	6,2
I0,680	7,0	4,6
I0,725	7,0	4,7
I0,762	I2,8	8,5
I0,813	II,7	7,8
I0,92	I3,2	8,8
II,05	5,2	3,5
II,09	II,2	7,5
II,20	7,3	4,8
II,26	6,0	4,0
II,34	8,9	5,9
II,43	II,2	7,4
II,51	I5,2	I0,I
II,67	4,4	3,0
II,71	3,5	2,3
II,81	II,5	7,7
II,90	9,2	6,2
I2,06	9,I	6,0
(I2,I6)	(8,7)	(5,8)
I2,27	4,6	(3,I)
I2,41	(4,5)	(3,0)

* $\gamma \sim I + 5/6 \sin^2 \theta$

** $g = 3/2$

I8 - Ar - 040

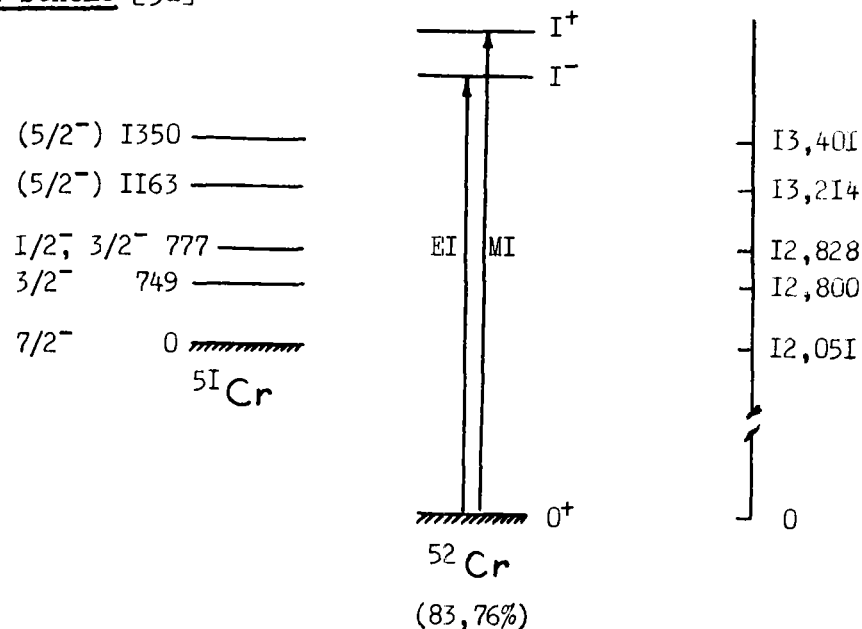
Radiation strength function for EI transitions

$$\langle \Gamma_{\gamma} / D \rangle = 8 \cdot 10^{-5} \quad [39].$$

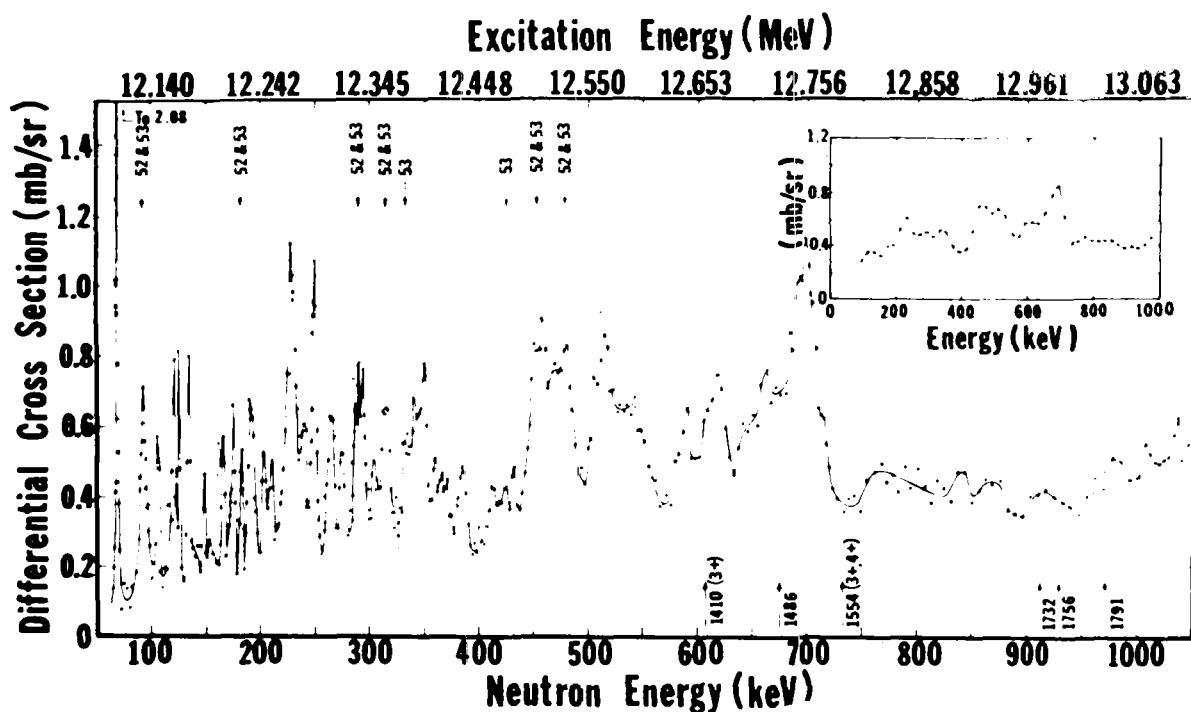
CHROMIUM-52

24 - Cr - 052

Level scheme [5d]



Differential cross-sections [27]



$$\begin{aligned} E_{\gamma}^{\max} &= 13.7 \text{ MeV} \\ \theta &= 135^\circ \end{aligned}$$

Sample - metal. Isotopic composition: ^{50}Cr : ^{52}Cr : ^{53}Cr : ^{54}Cr = 4.31:83.76:9.55:2.38.

24 - Cr - 052

Mass of chromium-52 ~ 214 g.

Resolution ~ 1.1 nsec/m.

The insert shows cross-sections averaged for a right-angled smoothing function of width 40 keV.

The arrows in the lower part of the diagram indicate the position of isobar-analogues of the lower levels of the ^{52}Cr nucleus. The figures beside the arrows represent values of J^π and of excitation energy of these levels.

The arrows in the upper part of the diagram indicate resonances associated with other chromium isotopes, and the figures are the corresponding mass numbers.

Resonance parameters [27]

E_n^{lab} (keV)	$g_\gamma \Gamma_{\gamma\gamma} \Gamma_n / \Gamma$ (eV)	GS or ES
68,2	0,69	GS
105	0,40	GS
121	0,71	GS
125	0,35	GS
133	0,60	GS
147	0,31	
166	0,50	GS
175	0,62	GS
191	0,95	GS
203	0,49	GS
210	0,43	GS
229	2,47	GS
238	0,71	GS
249	1,22	GS
264	0,95	GS
274	0,61	GS
286	0,55	
293	0,59	
341	0,78	GS
349	1,04	GS
385	0,66	GS

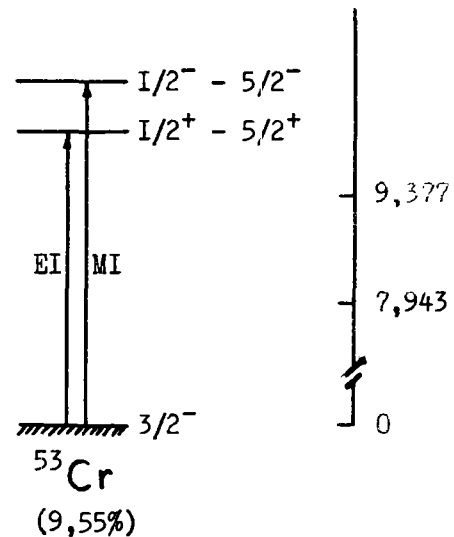
CHROMIUM-53

24 - Cr - 053

Level scheme [6d]

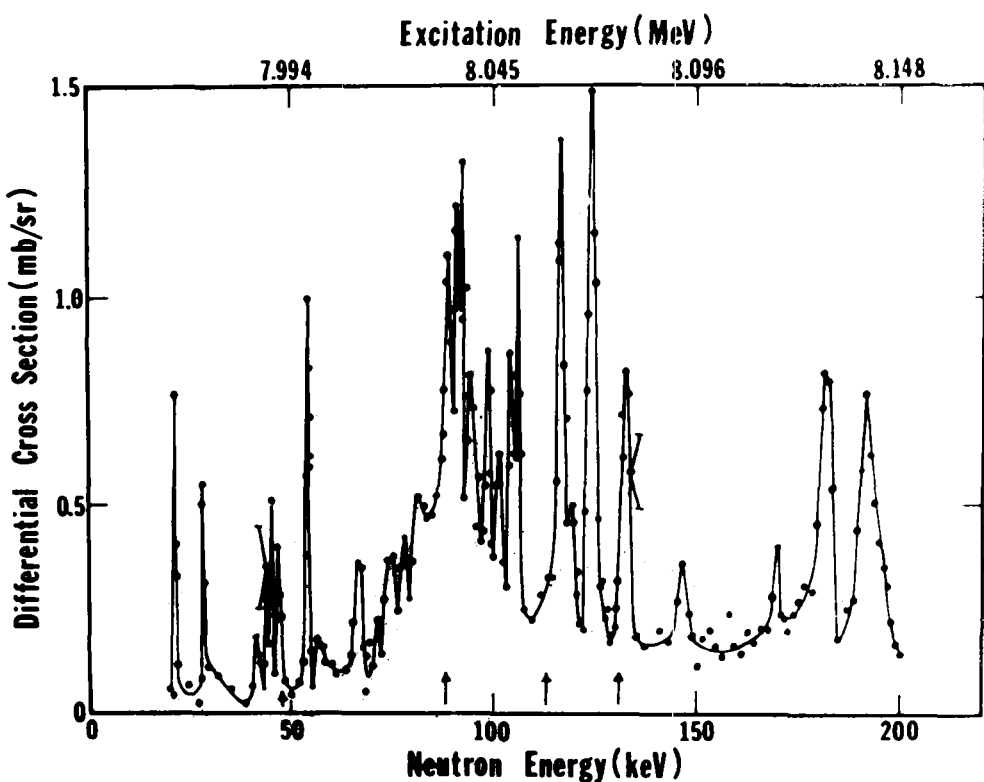
2^+ I434, I9 —————
 0^+ 0 

^{52}Cr



$(9,55\%)$

Differential cross-sections [27, 28]



$E_{\gamma}^{\max} = 11,5 \text{ MeV}$

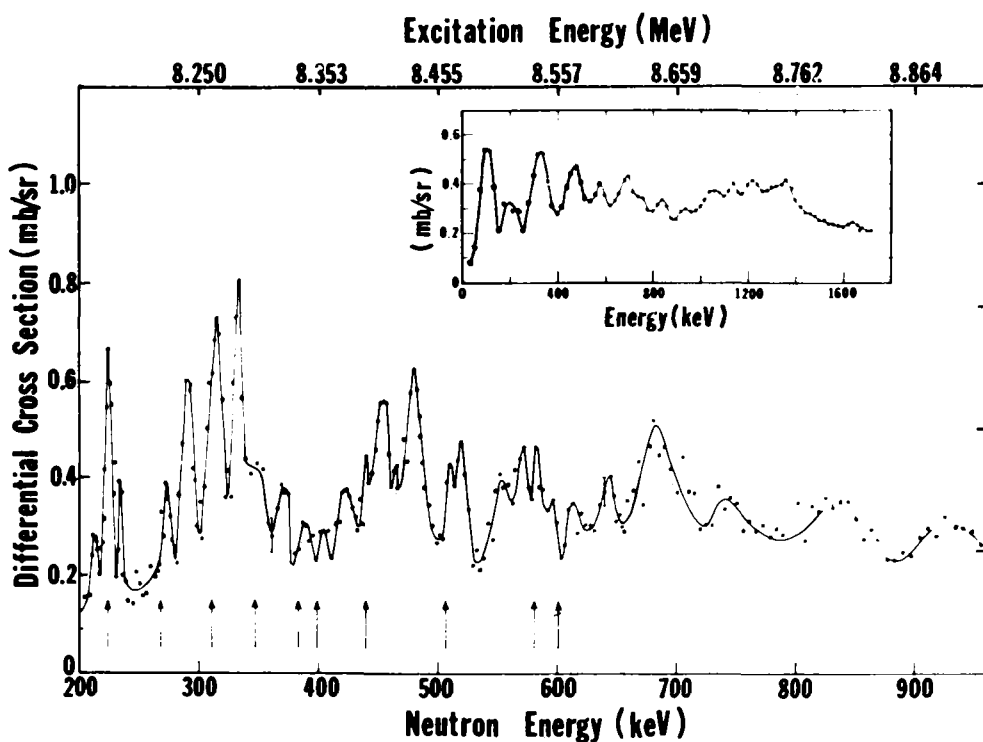
$\theta = 135^\circ$.

24 - Cr - 053

Resolution - 1.1 nsec/m

Sample - 52 g of Cr₂O₃. Isotopic composition: ⁵⁰Cr: ⁵²Cr: ⁵³Cr: ⁵⁴Cr = 0.82:3.37:95.56:0.25. Weight of chromium-53 - 41.5 g.

The arrows indicate the position of resonances with $J^\pi = 1/2^+$ which are known from the measured total cross-sections of chromium-52.

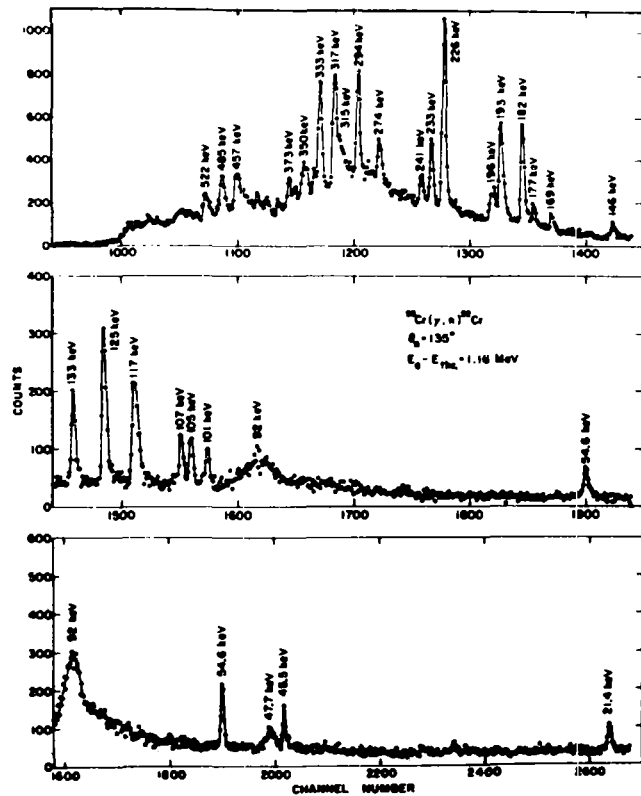


See subscripts to preceding diagram.

Range of higher neutron energies.

Cross-sections averaged for a right-angled smoothing function of width 40 keV are shown in the insert.

Photoneutron yield [29]



$E_{\gamma}^{max} = 9,1 \text{ MeV}$

$\theta = 135^{\circ}$

Sample - 64.4 g of Cr_2O_3 . Chromium-53 content - 96%.

Resolution - 1 nsec/m

Values of E_n^{lab} are shown near the peaks.

24 - Cr - 053

Resonance parameters

E_n^{lab} (keV)	[27]	[29]	$g_\gamma \Gamma_{\gamma^*} \Gamma_n / T$ (eV)	GS or ES	J^π	$\Gamma_{\gamma^*} \Gamma_n / T$ (eV)	E_n^{res} (keV)		
							[27]	[IIId]	[12d]
21,4	21,4	0,013				0,026 *	23,0	22,9	
28,3		0,031					30,3		
44,4		0,022					47,2		
45,5	45,5	0,034				0,009 *	48,4		
47,I		0,042			[I/2 ⁺]	0,17 **	50,I	51,0	50,2
	47,7				I/2 ⁺	0,179			
54,5	54,6	0,084	GS			0,046 *	57,8	57,8	
67,2		0,049					71,I		
89,0		0,38					94,0		
91,0		0,17					96,I		
	92				I/2 ⁺	I,275			
92,7		0,057					97,9		
94,4		0,25					99,6		
98,6		0,15					I04		
I02		0,11					I08	I07	
I04		0,13					I10	III	
I05					3/2 ⁻	0,075			
I06		0,10					I12		
I07	I07				3/2 ⁻	0,I43			
II7	II7	0,31	GS		I/2 ⁺	0,930	I23	I23,2	
I24		0,34	GS				I31	I30	I32
I25					3/2 ⁻	0,256			
I32		0,20	GS				I39		
I33					3/2 ⁻	0,I93			
I46					I/2 ⁻	0,234			
I47		0,065					I55		
I70		0,054					I79		
I75						0,046 *			
I82	I82	0,31	GS		I/2 ⁻	I,210	I91		
I91		0,35	GS				20I	I99	
I93					I/2 ⁻	I,I37			
I96					3/2 ⁻	0,I51			
212		0,084					223	224	
224		0,40	GS		[I/2 ⁺]	I,6 **	235	235	
226					I/2 ⁺	I,315			

24 - Cr - 053

E_n^{lab} (keV)	[27]	[29]	$g_{\gamma} \Gamma_{\gamma_0} \Gamma_n / \Gamma$ (eV)	GS or ES	J^{π}	$\Gamma_{\gamma_0} \Gamma_n / \Gamma$ (eV)	E_n^{res} (keV)		
							[27] [IId] [I2d]		
234	233	0,07			$I/2^-$	0,409	246	246	
	24I				$3/2^-$	0,069			
272		0,18	GS	$[I/2^+]$	$0,72$ **		285	28I	285,4
	274				$3/2^-$	0,077			
292		0,58	GS				306		
	294				$I/2^-$	0,748			
315	315	0,74	GS	$I/2^+$	0,184		330	326	33I,I
	317				$3/2^-$	0,395			
333	333	0,60	GS	$[I/2^-]$	I,324		349	349	
347		0,32		$[I/2^+]$	I,3 **		364	364	
	350				$3/2^-$	0,249			
371		0,20					389		
	373				$I/2^-$				
389		0,09		$[I/2^+]$	0,36 **		408	40I	
404		0,06		$[I/2^+]$	0,24 **		423	4I8	
422		0,24					443	442	
440		0,11					46I		
454		0,54	GS				475		
480		0,68	GS				502		
510		0,19	GS	$[I/2^+]$	0,76 **		533	530	
519		0,20	GS				543		

Comments:

The values of J^{π} given in square brackets in column 5 are taken from Refs [11d] and [12d].

* Values of $g_{\gamma} \Gamma_{\gamma_0} \Gamma_n / \Gamma$ are taken from Ref. [29].

** Values of Γ_{γ_0} are taken from Ref. [27].

Radiation strength function

$$\langle \Gamma_{\gamma_0} / D \rangle = (1,6 \pm 0,8) \cdot 10^{-5} \quad [27]$$

NATURAL IRON

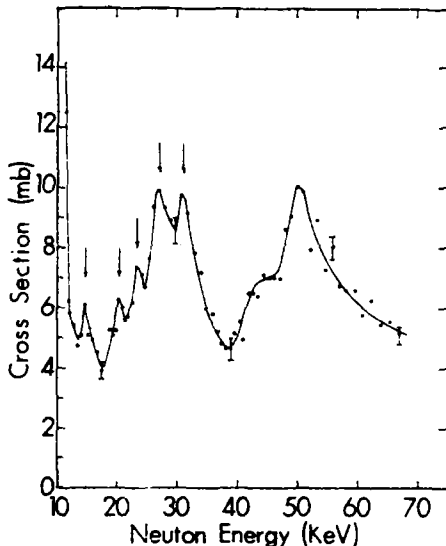
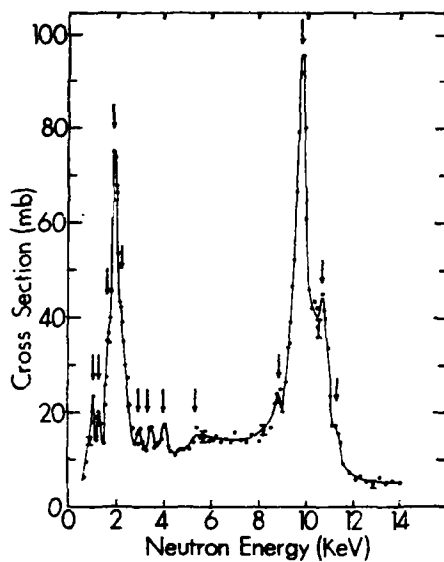
26 - Fe - ect.

Isotopic content

A	p [1d] (%)	Q _n [2d] (MeV)
54	5,84	13,62
56	91,68	11,21
57	2,17	7,642
58	0,31	10,047

Differential cross-sections

Results from Ref. [4]



$$E_{\gamma}^{\max} = 12,7 \text{ MeV}$$

$$\theta = 135^\circ.$$

Resolution - 15 nsec/m

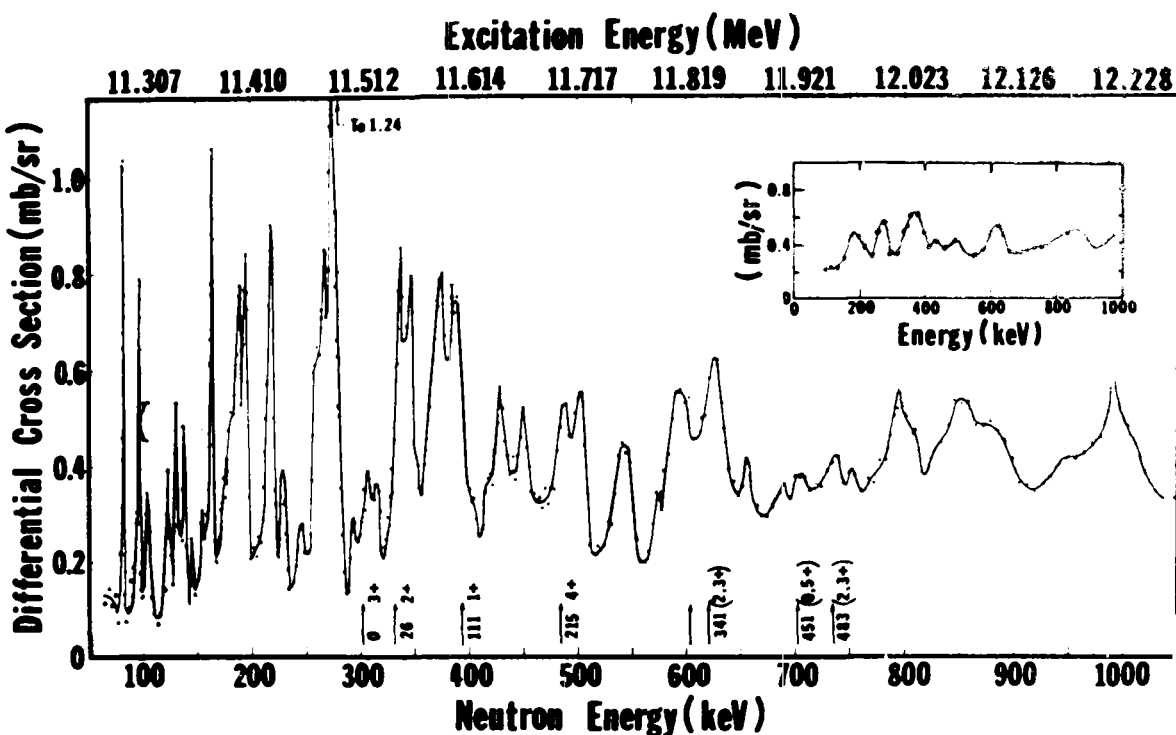
Sample - metal (disc of diameter 7.62 cm, $\delta = 1.25$ cm)

The arrows indicate peaks for which data are given in the table.

The uncertainty on the axis of ordinates $\approx 30\%$.

26 - Fe - ect.

Results from Ref. [27]



$$E_{\gamma}^{\max} = 12.7 \text{ MeV}$$

$$\theta = 135^\circ.$$

Resolution - 1.1 nsec/m

Sample - metal. Weight of iron-56 - 416 g

The insert gives cross-sections averaged for a right-angled smoothing function of width 40 keV.

Control measurements at $E_{\gamma}^{\max} = 11.45$ MeV show that the main part of the observed structure is due to transitions to the ground state of the residual ^{55}Fe nucleus.

The arrows indicate the position of isobar-analogues of low-lying levels of manganese-56. Values of J^π and of excitation energy for these low-lying levels are given alongside the arrows.

26 - Fe - ecr.

Resonance parameters [4]

E_n^{lab} (keV)	$\Gamma \approx \Gamma_n$ (eV)	$g\Gamma_{\gamma_0}$ (eV)	σ_0 (mbarn)
I,05			
I,25			
I,65			
I,92	415	0,80	73
2,20			
2,95			
3,40			
4,00			
5,35			
8,80			
9,80*	560*	I,93	96
I0,65			
II,30			
I4,70			
2I,0			
23,5			
27,0			
3I,0			

* According to later work (Ref. [27]), $E_n^{\text{lab}} = 9.63$ keV and $\Gamma \approx \Gamma_n = 160$ eV.

Comments:

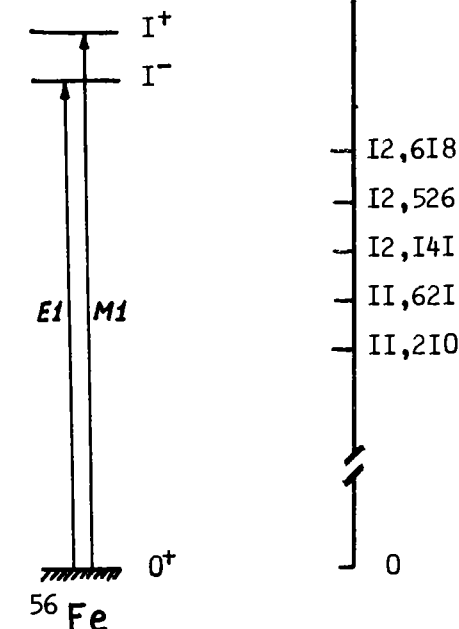
- (1) It is assumed that the strong levels at $E_n^{\text{lab}} = 1.92$ and 9.80 keV correspond to iron-56, and this is supported by a comparison of the measurements with $E_n^{\text{max}} = 12.7$ and 11.6 MeV. In this case $J^\pi = 1^-$ and $\Gamma_{\gamma_0} = 2/3(g\Gamma_{\gamma_0})$!
- (2) The remaining peaks may be associated either with iron-57 levels or with p-resonances of iron-56.

IRON-56

26 - Fe - 056

Level schemes [7d]

5/2⁻, 7/2⁻ I408,4
5/2⁻, 7/2⁻ I3I6,4
5/2⁻ 93I,2
I/2⁻ 4II,4
3/2⁻ 0
⁵⁵Fe



(91,68%)

Differential cross-sections

See data obtained for natural mixture of isotopes.

Radiation strength function

$$\langle \Gamma_{\gamma^*} / D \rangle = 3,5 \cdot 10^{-5} \quad [4].$$

26 - Fe- 056

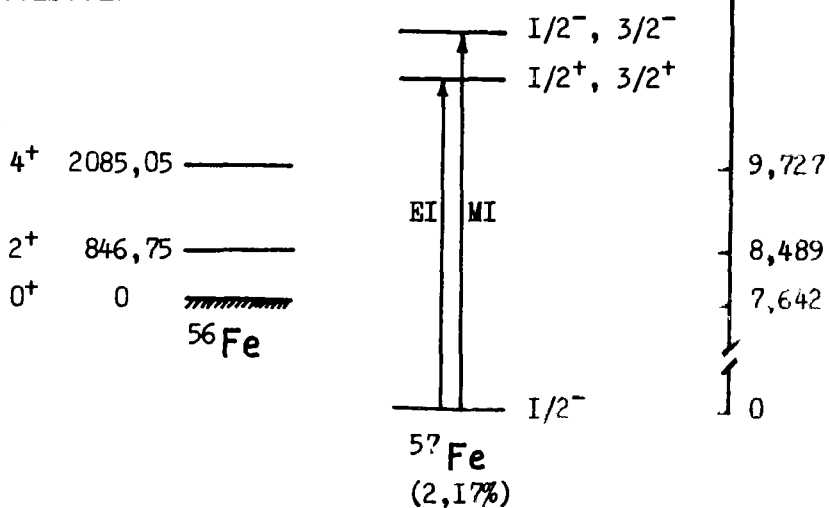
Resonance parameters [27] (See also data for natural mixture of isotopes)

E_n^{lab} (keV)	$g_s \Gamma_{\gamma\gamma} / \Gamma$ (eV)	GS or ES
83,I	0,30	GS
97,6	0,47	GS
105	0,30	
124	0,22	GS
132	0,23	GS
138	0,29	GS
164	0,74	GS
189	0,73	GS
195	0,80	GS
218	1,27	GS
228	0,31	GS
267	0,91	GS
274	1,84	GS
307	0,47	
316	0,29	
338	1,20	GS
347	1,13	GS
374	2,15	GS
388	1,64	GS
430	1,04	GS
450	0,95	GS
488	1,19	GS
502	1,03	GS
543	0,97	GS
576	0,34	
594	1,89	GS
627	2,30	GS
705	0,37	

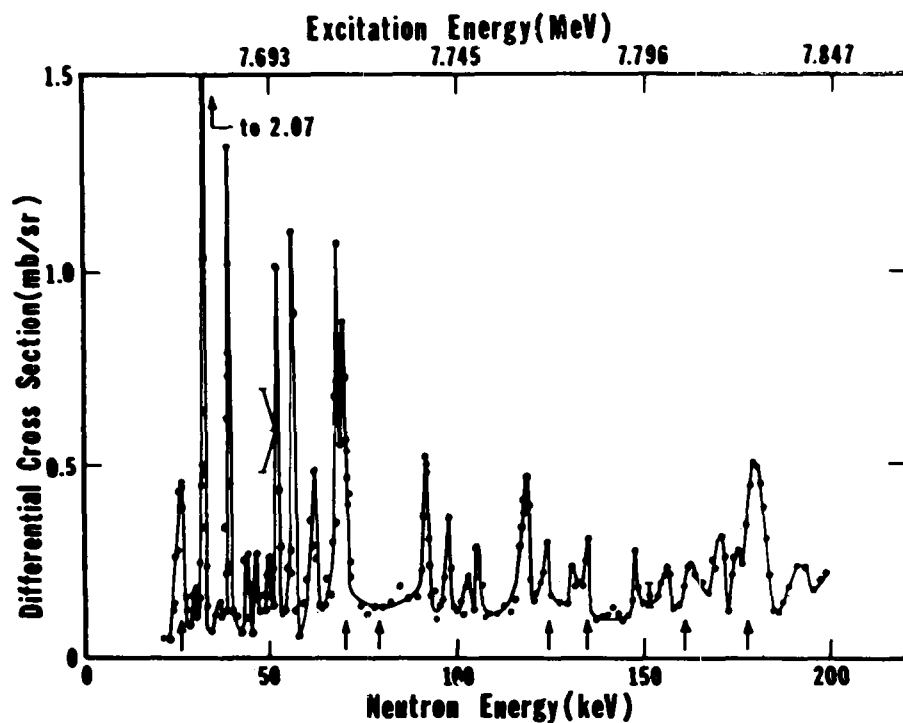
IRON-57

26 - Fe - 057

Level scheme [8d]



Differential cross-sections [27, 28]



$$E_{\gamma}^{\max} = 11.5 \text{ MeV}$$

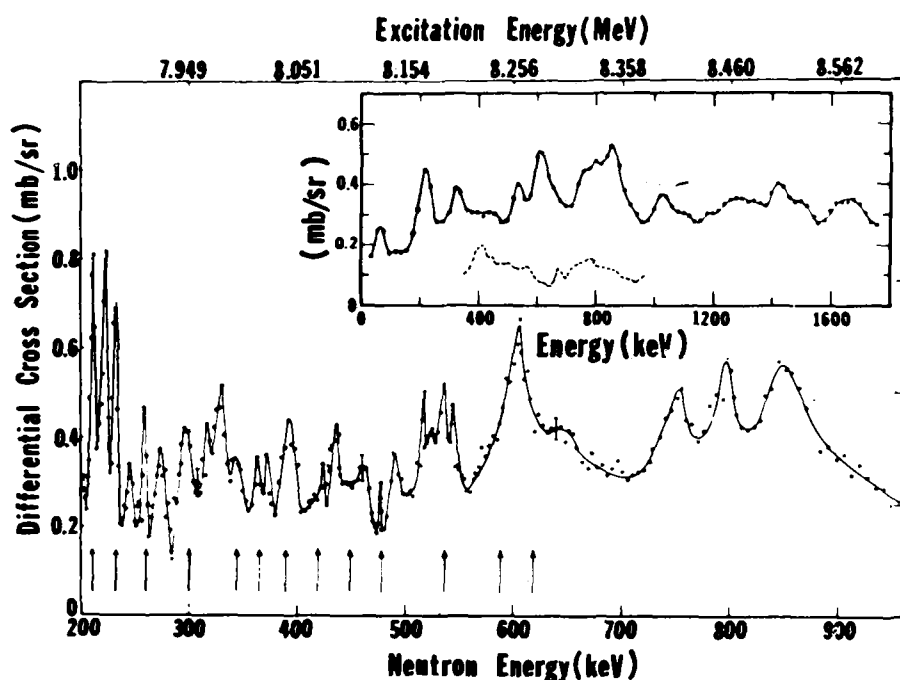
26 - Fe - 057

$\theta = 135^\circ$

Resolution - 1.1 nsec/m

The arrows indicate resonances with $J^\pi = 1/2^+$ found in studies on the $^{56}\text{Fe}(n,n)^{56}\text{Fe}$ reaction [5].

Sample - Fe_2O_3 . Isotopic composition: $^{54}\text{Fe}:^{56}\text{Fe}:^{57}\text{Fe}:^{58}\text{Fe} = 0.20:9.25:90.42:0.13$. Weight of iron-57 - 43.3 g

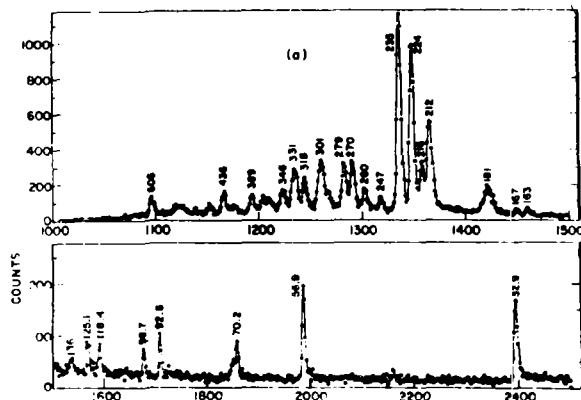


The continuous line in the insert gives cross-sections averaged for a right-angled smoothing function of width 40 keV.

The dotted line gives cross-sections of the $^{66}\text{Fe}(n,n)$ reaction.

26 - Fe - 057

Photoneutron yield [29, 34]



$$E_e - E_{\gamma}^{\text{th}} = 0.81 \text{ MeV} \quad (E_{\gamma}^{\text{max}} = 8.45 \text{ MeV})$$

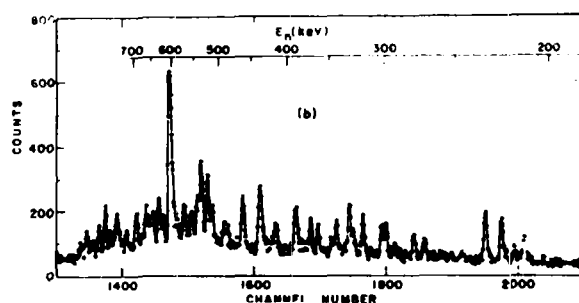
$\theta = 90^\circ$

Sample - 39.7 g of Fe_2O_3 . Iron-57 enrichment - 90.4%.

No account was taken of variations in the sensitivity of the detector with neutron energy or of the energy dependence of the gamma-radiation flux.

Values of E_n^{lab} (keV) are indicated alongside the resonances.

Flight path lengths - 9 m, $\tau = 6$ nsec.



$$E_e - E_e^{\text{th}} = 1.06 \text{ MeV} \quad (E_{\gamma}^{\text{max}} = 8.6 \text{ MeV}).$$

See subscript to Fig. (a).

26 - Fe - 057

Resonance parameters

E_n^{lab} (keV)	$g_F \Gamma_\gamma \Gamma_n / T$ (eV)	GS or ES	J^π		$\Gamma_\gamma \Gamma_n / T$ (eV)	Γ_γ (eV)	E_n^{res} (keV)			
[27]	[29]	[27]	[11d]	[29]	[29]	[27]	[27]	[11d]	[16d]	
26,0	26,7	0,084		$I/2^+$	$I/2^+$	0,II2	0,I7	27,7	28	27,7
32,3	32,9	0,II			$I/2^-$	0,I80		34,3		34,I
38,7		0,055						4I,0		
51,8		0,080						54,7		
56,2	56,9	0,I2			$I/2^-$	0,22I		59,4		59,0
61,5		0,067						64,9		63,I
68,2		0,I0						7I,8		
69,I	70,2	0,I2		$I/2^+$	$I/2^+$	0,082	0,24	72,8	74	72,6
91,6	92,6	0,069				0,045*		96,3		95,9
97,7	98,7	0,03I				0,042		I02,7		I02
I06		0,022						III		II2
I19	I18,4	0,094	GS		$I/2^+$	0,II9		I25		
I24	I25,I	0,028		$I/2^+$	$I/2^+$	0,I05	0,056	I30	I3I	I29
I35	I36	0,036		$I/2^+$	$I/2^+$	0,068	0,072	I4I	I42	
I48		0,027						I55		
I56		0,044						I63	I64	
I62	I63	0,059		$I/2^+$	$I/2^+$	0,066	0,I2	I70	I69	
	I67					0,032*				
I7I		0,072						I79		
I79	I8I	0,2I	GS	$I/2^+$	$I/2^+$	0,423	0,42	I87	I87	
I92		0,050						20I		
2I2	2I2	0,36	GS	$I/2^+$	$I/2^+$	0,683	0,72	222	220	
	2I6				$I/2^-$	0,I30				
223	224	0,40			$3/2^-$	0,364		233		
232	235	0,26	GS	$I/2^+$	$3/2^-$	0,382	0,52	243	244	

26 - Fe - 057

E_n^{lab} (keV)	$g_{\gamma} \Gamma_{\gamma} \Gamma_n / \Gamma$ (eV)	GS or ES	J^{π}	$\Gamma_{\gamma} \Gamma_n / \Gamma$ (eV)	Γ_{γ} (eV)	E_n^{res} (keV)	
[27]	[29]	[27]	[11d]	[29]	[27]	[11d]	[16d]
245	247	0,072			0,030*		
259	260	0,II	I/2 ⁺	0,046*	0,22	27I	273
	270		3/2 ⁻	0,090			
274		0,I5				286	
	278		I/2 ⁻	0,208			
299		0,32	I/2 ⁺		0,64	3I2	3I5
330		0,32				345	
393		0,3I				4I0	406

* Values of $g_{\gamma} \Gamma_{\gamma} \Gamma_n / \Gamma$.

Radiation strength function

$$\langle \Gamma_{\gamma} / D \rangle = (1,1 \pm 0,6) \cdot 10^{-5} \quad [27].$$

Doorway states

A group of strong resonances is observed at energies around 50 keV [28]. Since from studies on ^{56}Fe only two S-resonances are known in this range, values $J^{\pi} = 3/2^+$ are assigned to all the remaining resonances. The origin of this group of levels is related to the doorway states.

A second group of resonances with $J^{\pi} = 1/2^+$ is observed at energies around 250 keV [28]. For this group the rank correlation coefficient for values of Γ_n^0 is $Q = 0.20$, so that one cannot exclude the possibility that the group may be attributable to statistical fluctuations.

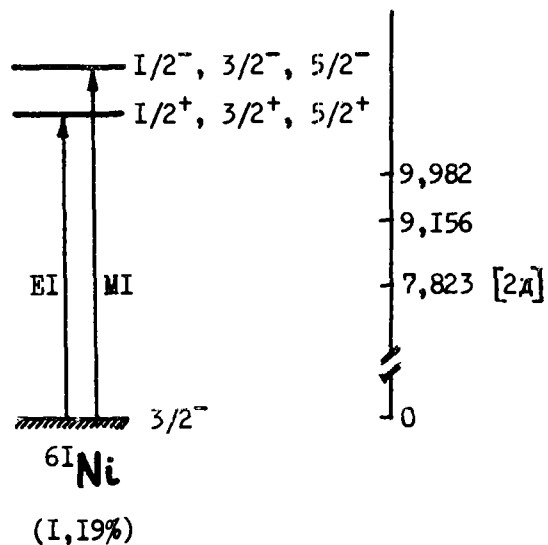
There is an anomalous concentration of the strength of MI-transitions in three resonances at 224 keV ($3/2^-$), 235 keV ($3/2^-$) and 606 keV ($1/2^-$), which may be due to the existence of doorway states of type $(f_{5/2}) (f_{7/2})^{-1}$ [34].

NICKEL-61

28 - Ni - 06I

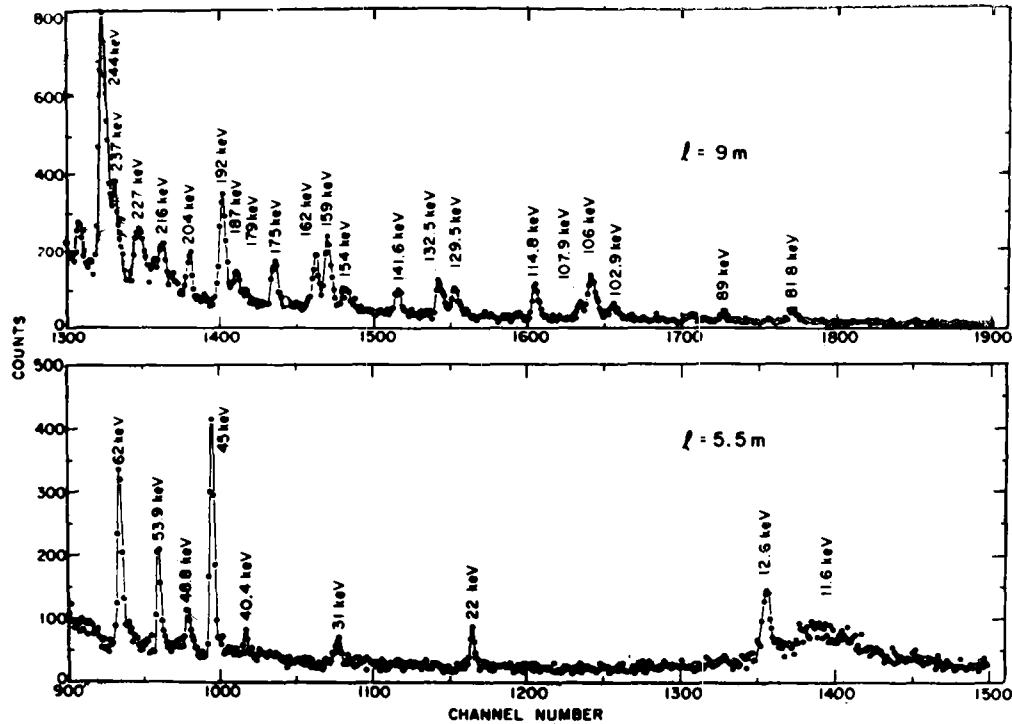
Level scheme [1d]

2^+ 2159 —
 2^+ 1332,5 —
 0^+ 0 —
 ^{60}Ni



(I, I9%)

Photoneutron yield [29]



$E_{\gamma}^{\max} = 8,9 \text{ MeV}$

$\theta = 90^\circ$

The values of E_n^{lab} are indicated above the peaks.

28 - Ni- 06I

Resonance parameters [29]

E_n^{lab} (keV)	J^π	$\Gamma_{\gamma\gamma} \Gamma_n / \Gamma$ (eV)
II,6	$1/2^+$	0,367
I2,6	$1/2^-$	0,040
22,0	$3/2^-$	0,020
31,0	$3/2^-$	0,018
40,4	$1/2^+$	0,018
45,0	$1/2^-$	0,166
48,8	$3/2^-$	0,034
53,9	$1/2^-$	0,092
62,0	$3/2^-$	0,189
81,4	$3/2^-$	0,093
89,0		0,014 *
92,6	$1/2^+$	0,102
I02,9	$1/2^+$	0,209
I06,0	$1/2^-$	0,419
I07,9		0,032 *
II4,8	$3/2$	0,205
I29,5	$1/2^-$	0,256
I32,5	$1/2^-$	0,314
I41,6	$1/2^-$	0,148
I54	$1/2^+$	0,166
I59	$1/2^-$	0,216
I62	$3/2^-$	0,231
I75		0,067 *
I79	$1/2^+$	0,062
I87	$3/2^-$	0,165
I92	$1/2^+$	0,557

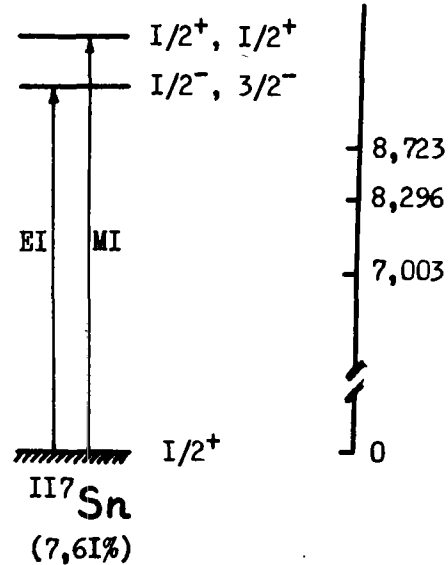
* The value of $\Gamma_{\gamma\gamma} \Gamma_n / \Gamma$.

TIN-117

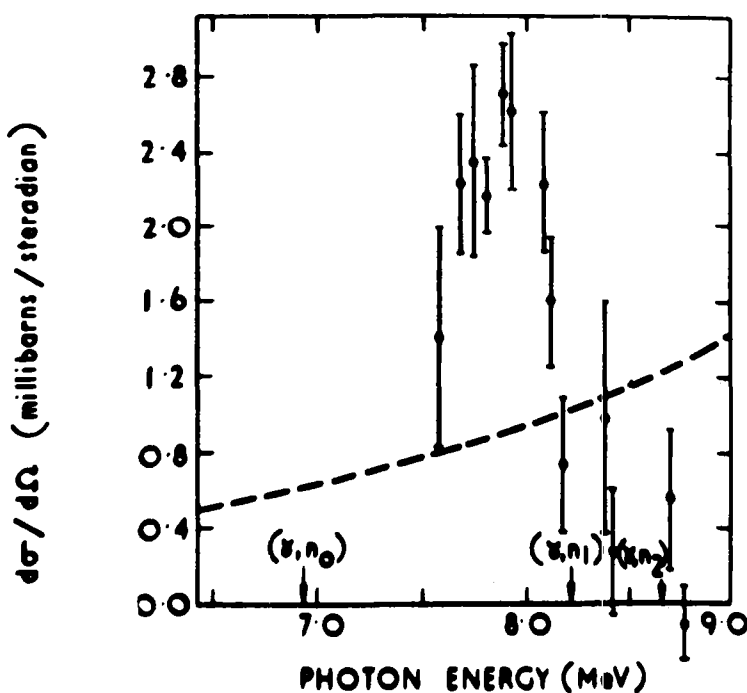
50 - Sn- 117

Level scheme [42]

(0⁺) I720 —————
2⁺ I293 —————
0⁺ 0
II⁶Sn



Differential cross-sections [42]



E_{γ}^{\max} = 9.2 MeV.

θ = 130°

Resolution - 3 nsec/m

Uncertainty along the axis of ordinates \approx 25%.

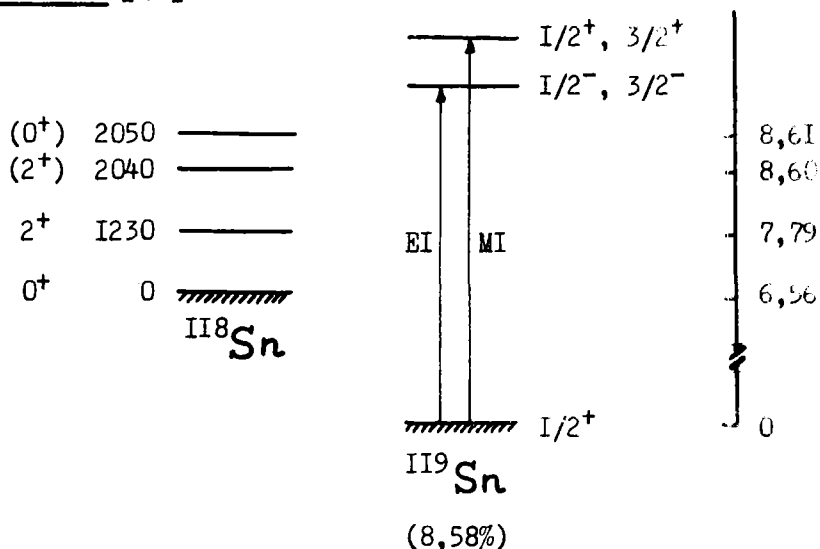
The vertical lines indicate statistical errors only.

The dotted line represents extrapolation of the giant resonance "tail".

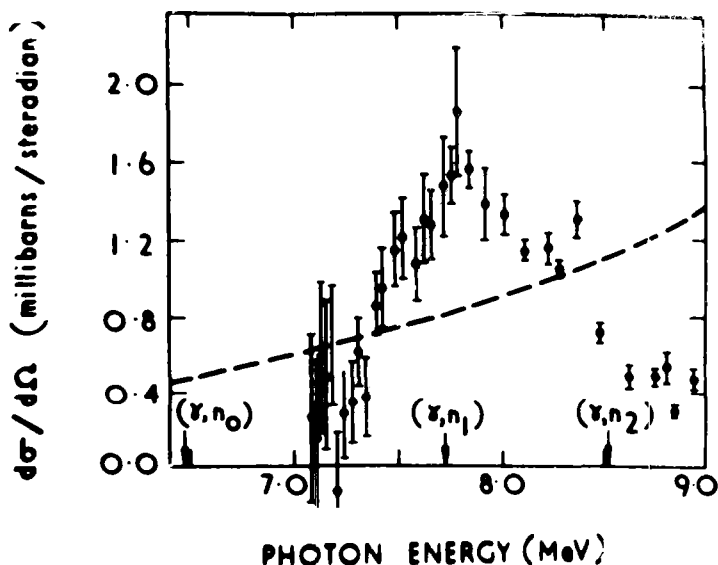
TIN-119

50 - Sn - I19

Level scheme [42]



Differential cross-sections [42]



E_{γ}^{\max} up to 9.2 MeV

$\theta = 130^\circ$

Resolution - 3 nsec/m

Uncertainty on axis of ordinates $\approx 25\%$

Vertical lines indicate statistical errors only

The dotted line represents extrapolation of the giant resonance "tail"

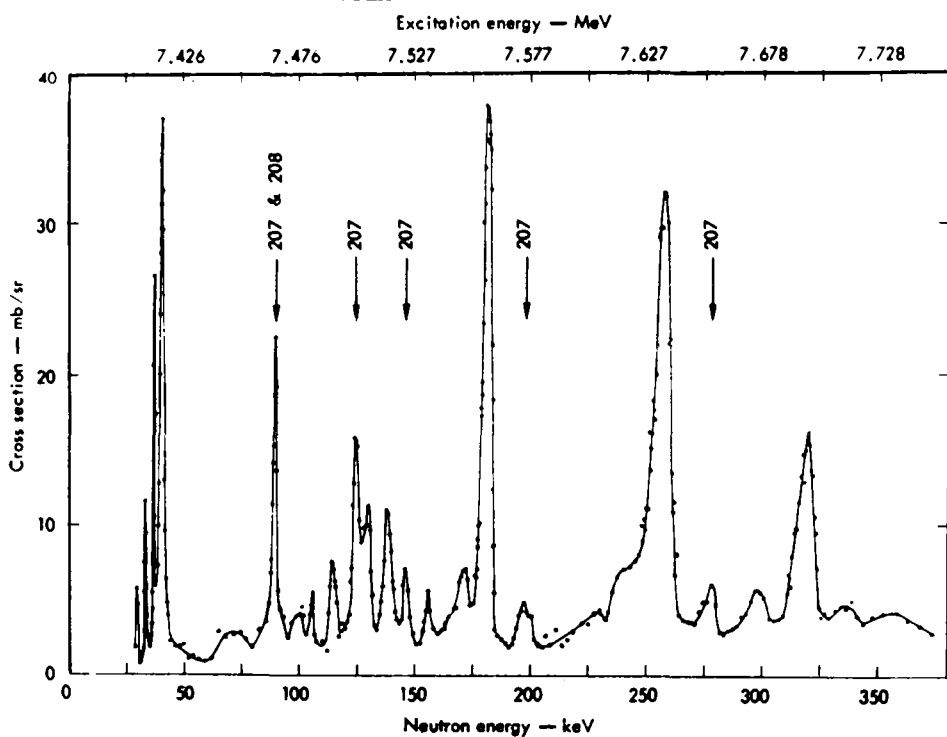
NATURAL LEAD

82 - Pb - nat.

Isotopic content p and neutron binding energy Q_n

A	P (%)		Q_n (MeV) [2.d]
	[Id]	[27]	
204	1,37	1,48	8,38
206	25,0	23,6	8,13
207	21,2	22,6	6,73
208	52,4	52,3	7,38

Differential cross-sections [14]



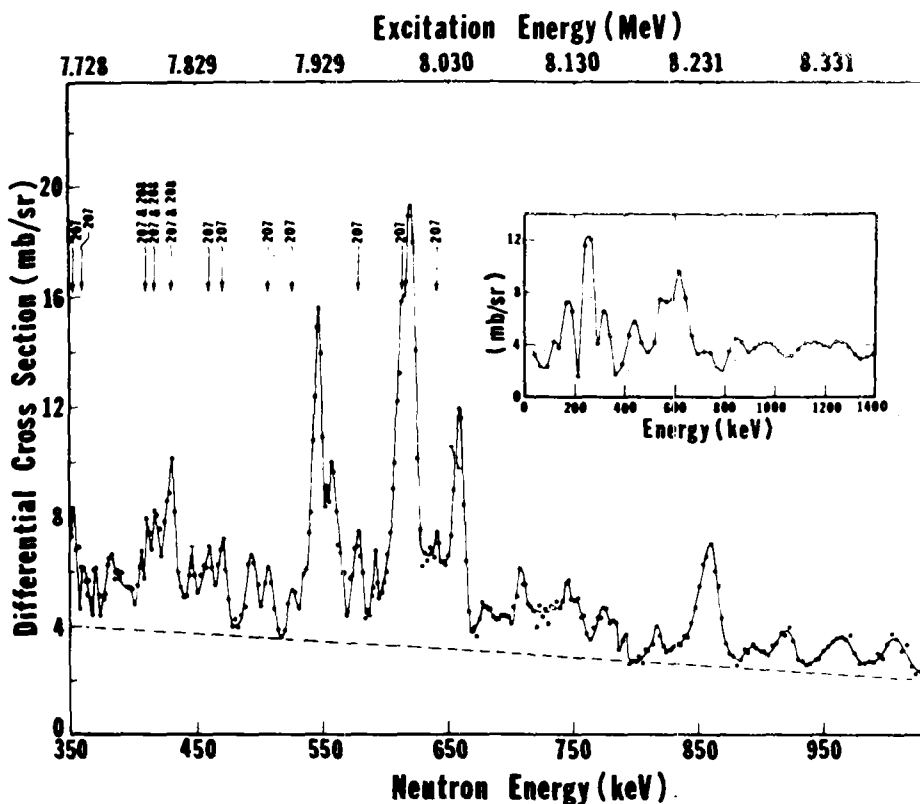
$$E_{\gamma}^{\max} = 9.0 \text{ MeV}$$

$$\theta = 135^\circ$$

The arrows indicate resonances corresponding to lead-207; the remaining resonances correspond to lead-208.

82 - Pb - nat

Differential cross-sections [27]



$$E_{\gamma}^{\max} = 10.0 \text{ MeV}$$

$$\theta = 135^\circ$$

Resolution = 0.6 nsec/m

Sample - metal

Weight of lead-208 - 127 g

The dotted line represents the estimated background

The arrows indicate resonances corresponding to lead-207;
the remaining resonances correspond to lead-208

The insert gives cross-sections averaged for a right-angled smoothing
function of width 40 keV.

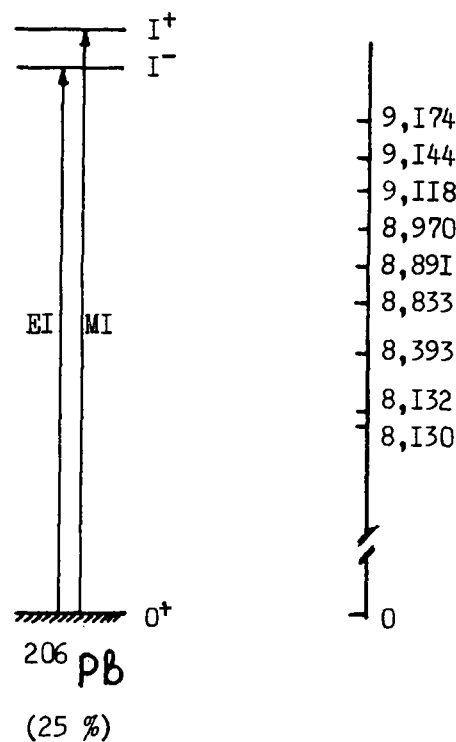
LEAD-206

82 - Pb- 206

Level scheme [1d]

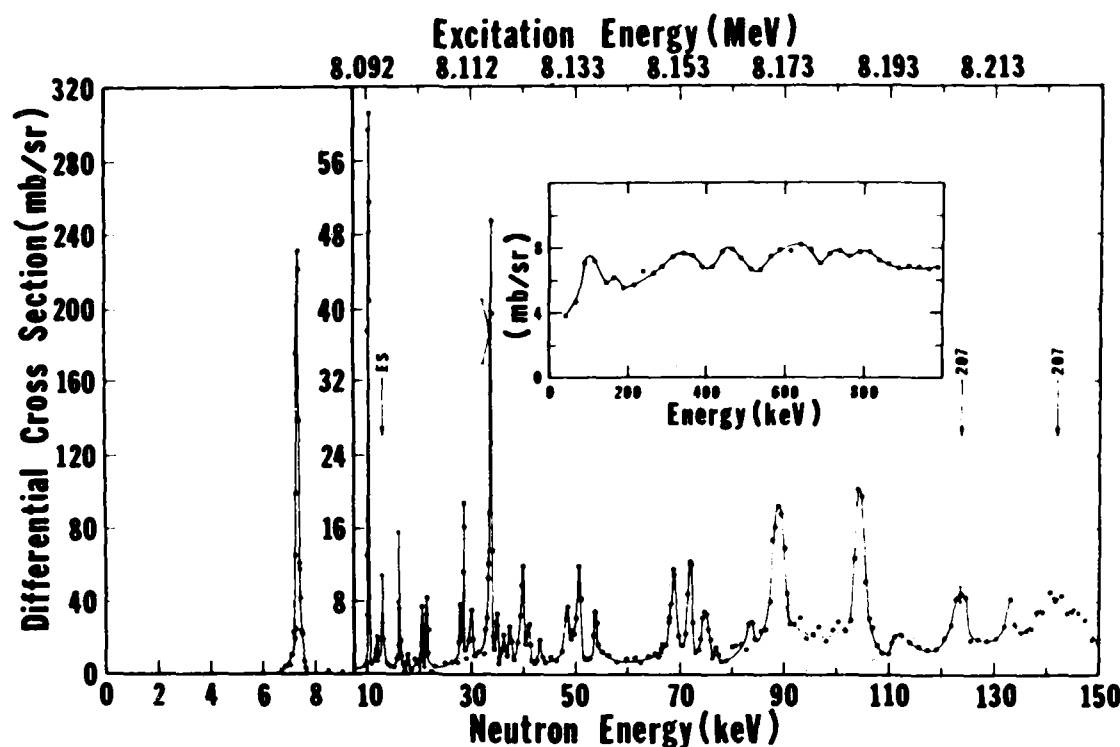
(5/2 ⁻)	1043,7
13/2 ⁺	1013,8
9/2 ⁻	987,6
	840
(3/2 ⁻)	761
7/2 ⁻	703,3
3/2 ⁻	262,8
1/2 ⁻	2,3
5/2 ⁻	0

205 Pb



(25 %)

Differential cross-sections [27]



82 - Pb - 206

E_{γ}^{\max} = 10.0 MeV

θ = 135°

Resolution = 1.6 nsec/m

Isotopic composition of sample: ^{204}Pb : ^{206}Pb : ^{207}Pb : ^{208}Pb = 0.085:88.38
8.57:2.97. Weight of lead-206 - 197 g.

The insert gives the cross-section averaged for a right-angled smoothing function of width 40 keV.

Resonances related to the isotope lead-207 and the peak corresponding to the transition to the excited state of the residual nucleus are indicated by arrows.

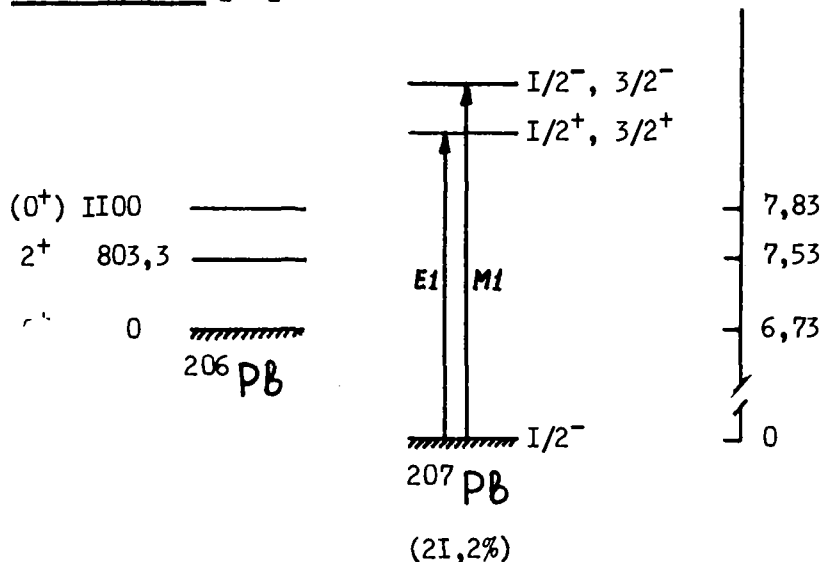
Resonance parameters [27]

E_n^{lab} (keV)	$g_{\gamma} \Gamma_{\gamma_0} \Gamma_n / \Gamma$ (eV)	GS or ES
I,5	0,4	GS
7,3	3,4	GS
10,3	I,I	GS
12,9	0,I2	ES
16,I	0,40	GS
28,5	0,54	
33,7	2,5	GS
40,0	0,86	
50,7	I,3	GS
53,6	0,52	
68,9	I,5	
72,I	I,4	
75,I	0,90	
88,9	4,5	
I04	4,9	

LEAD-207

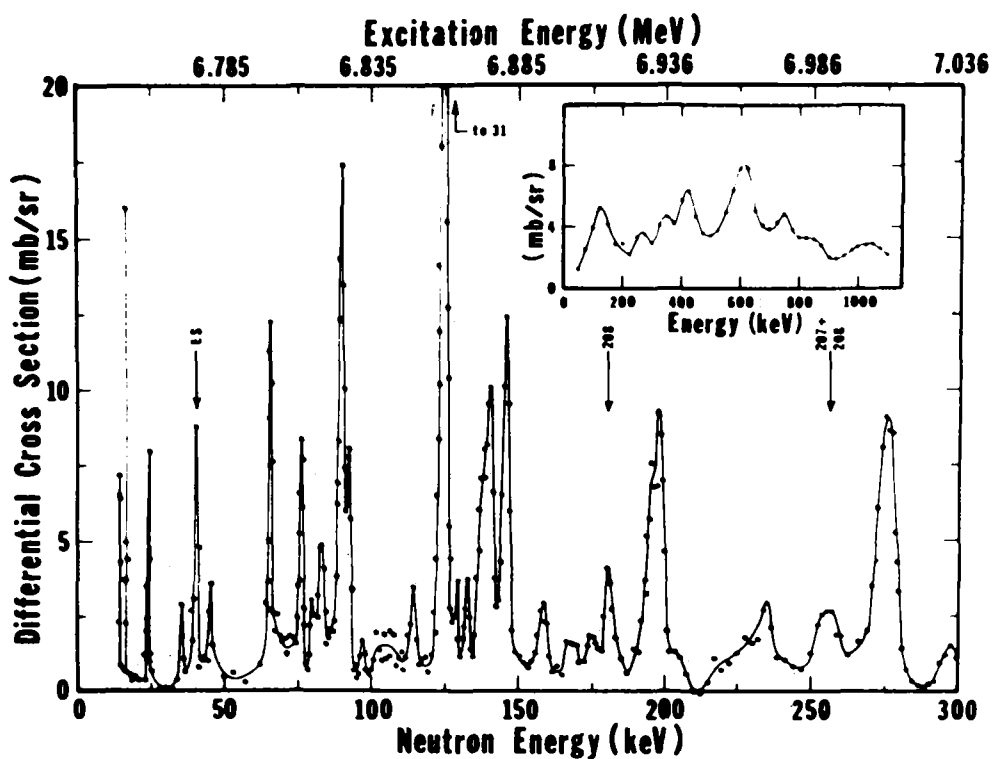
82 - Pb - 207

Level scheme [1d]



(2I, 2%)

Differential cross-sections [27, 28]



$E_{\gamma}^{\text{max}} = 8,4 \text{ MeV}$

$\theta = 135^0$.

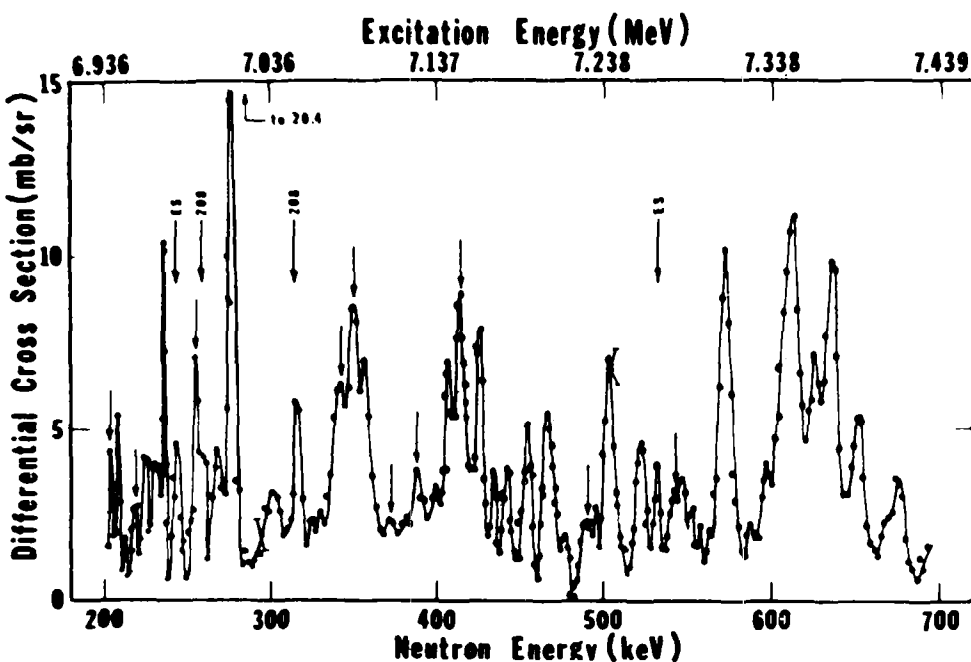
82 - Pb - 207

Isotopic composition of sample: ^{204}Pb : ^{206}Pb : ^{207}Pb : $^{208}\text{Pb} = 0.02$:
2.16: 92.36: 5.48. Weight of lead-207 - 132 g.

The insert gives cross-sections measured for a right-angled smoothing function of width 40 keV.

Arrows indicate resonances related to other lead isotopes and the peak corresponding to the transition to an excited state of the residual nucleus.

Resolution - 1.1 nsec/m.



$$E_{\gamma}^{\max} = 9.8 \text{ MeV}$$

$$\theta = 135^\circ$$

For isotopic content of sample, see above.

Resolution - 0.7 nsec/m

The arrows without figures indicate 10 resonances with $J^\pi = 1/2^+$.

Arrows with figures have the same meaning as in the previous figure.

Resonance parameters [27, 28]

E_n^{lab} (keV)	$g_F \Gamma_{\gamma_0} \Gamma_n / \Gamma$ (eV)	GS or ES	J^π	Γ_{γ_0} (eV)	E_n^{res} (keV)			
					[27]	[I3d]	[I4d]	[I5d]
3,3 *	0,07	GS			3,4			
II,2 *	0,054	ES						
I2,I *	0,03	GS			I2,3			
I4,3	0,34	ES						
I6,2	0,21	GS	$I/2^-$ [I3d]	0,42	I6,5	I6,5		
I9,8 *	0,08	GS			20,I			
24,9	0,71	GS	$3/2^-$ [I3d]	0,81	25,3	25		
35,8	0,97		$3/2^-$ [I3d]	I,I	36,4	35		
40,7	5,0	ES						
45,I	I,2		$3/2^-$ [I3d]	I,3	45,8	46		
65,7	I,6	GS	$I/2^+$ [I3d]	3,2	66,6	66		
76,I	I,I	GS			77,I			
82,6	I,I				83,8		85	
90,0	3,I	GS			91,2			
92,5	0,88				93,8			
97,0	0,30				98,3			
II4	0,82	GS			II5			
I25	6,6	GS			I27		I26	
I33	0,86				I35			
I40	4,0	GS			I42			
I46	2,9	GS			I48			
I59	I,I				I6I		I6I	
I68	0,78	GS			I70			
I75	0,78	GS			I77			
I96	I,9	GS			I98		I98	I97
I98	2,8	GS			200			
205	0,63		$I/2^+$ [I4d]	I,27	208		207	

Resonance parameters [27, 28] continued

E_n^{lab} (keV)	$g_\gamma \Gamma_{\gamma^*} \Gamma_n / \Gamma$ (eV)	GS or ES	J^π	Γ_{γ^*} (eV)	E_n^{res} (keV)			
					[27]	[I3d]	[I4d]	[I5d]
217	0,57		$I/2^+ [I4d]$	I,I3	220		219	
234	1,9	GS				237		
242	3,1	ES						
253	2,4	GS	$I/2^+ [I4d]$	4,74	256		256	
276	6,3	GS			279		278	
301	2,8				305			
342	4,?		$I/2^+ [I4d]$	9,42	346		348	
350	5,1		$I/2^+ [I4d]$	I0,26	354		355	
356	4,2				360			
374	0,88		$I/2^+ [I4d]$	I,75	379		383	
391	2,9		$I/2^+ [I4d]$	5,76	396		396	
407	4,0	GS			412			
416	4,7	GS	$I/2^+ [I4d]$	9,48	421		422	
426	4,1	GS			431			
454	2,5				459		460	
466	4,2				472		473	
488	0,94		$I/2^+ [I4d]$	I,88	494		495	
503	4,7				509		511	
523	3,7				529			
533	3,4	ES						
543	1,5		$I/2^+ [I4d]$	2,90	549		550	
572	8,5	GS			578			

*/ Data taken from Ref. [7].

Radiation strength function

$$\langle \Gamma_{\gamma^*} / D \rangle = (13 \pm 7) \cdot 10^{-5} \quad [27].$$

Doorway states [28]

The rank correlation coefficient ρ and momentum correlation coefficient r were found for ten $1/2^+$ resonances in the neutron energy range 200–550 keV for the values of Γ_{γ^*} and Γ_n^0 from Ref. [14d]:

$$\rho = 0,60 \quad \text{and} \quad r = +0,44.$$

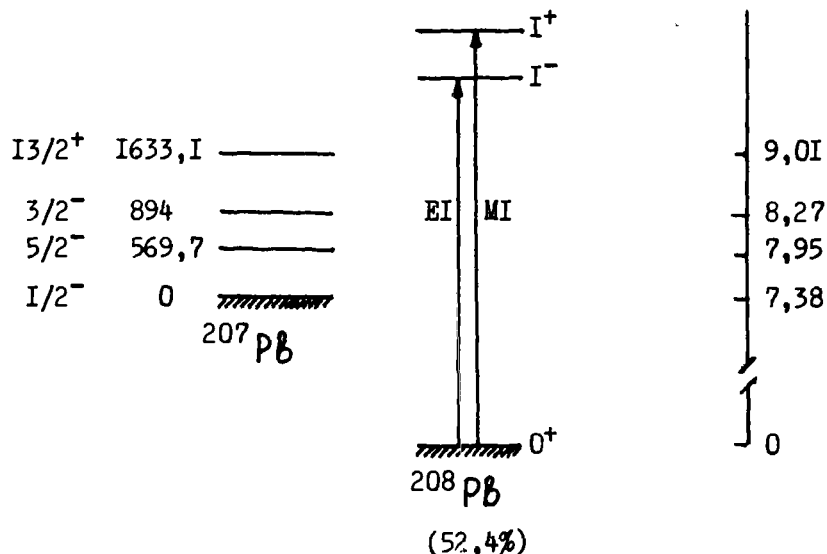
On the basis of this result it was concluded that there is a 0.964 probability of a correlation between the values of Γ_{γ^*} and Γ_n^0 .

This may be explained by the assumption that there exists a doorway state with a radiation width of 36.5 eV.

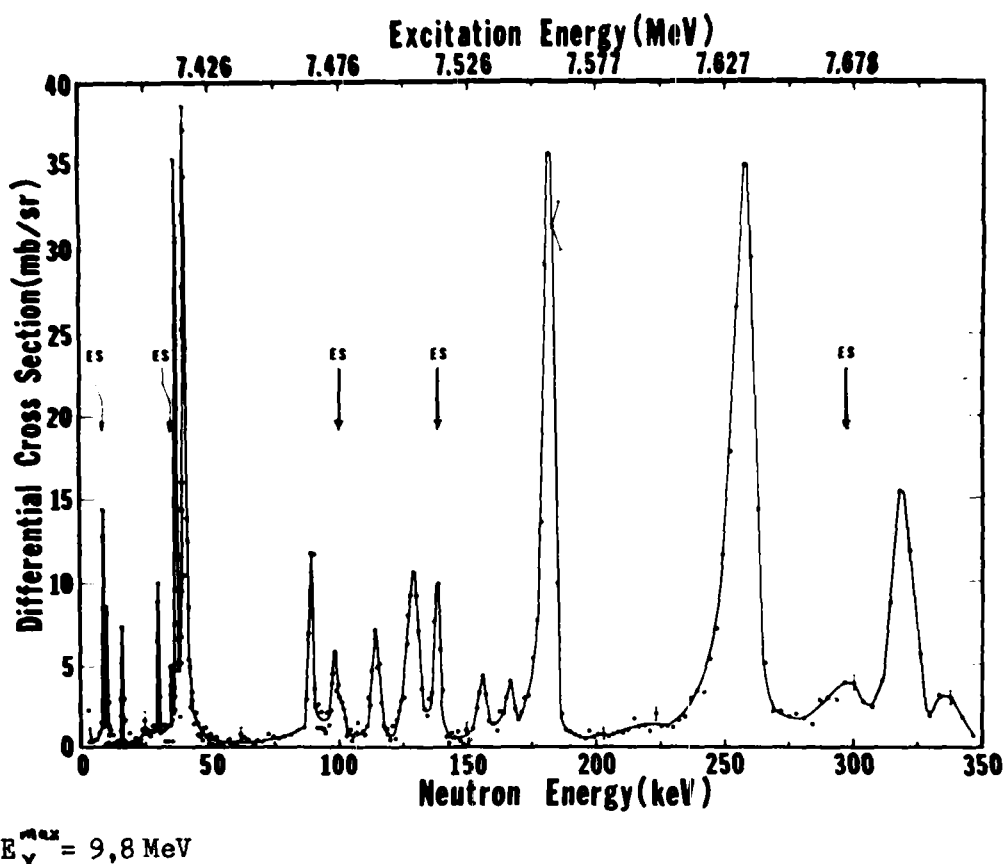
LEAD-208

82 - Pb - 208

Level scheme [1d]



Differential cross-sections [27, 28]



82 - Pb - 208

$\theta = 135^\circ$.

Resolution - 1.6 nsec/m

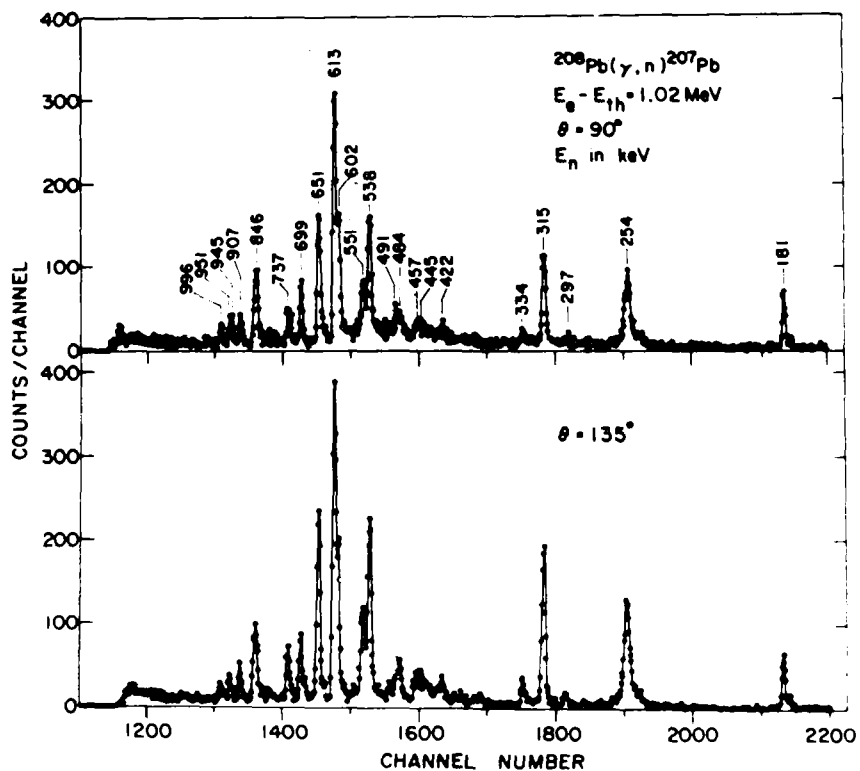
Sample - metal

Isotopic composition: ^{204}Pb : ^{206}Pb : ^{207}Pb : $^{208}\text{Pb} = 0.05$: 0.2: 0.05: 99.75.

Weight of lead-207 - 117 g

The arrows indicate resonances corresponding to transitions to excited states of the residual nucleus (from control measurements for $E_\gamma^{\max} = 7.8$ and 8.1 MeV).

Photoneutron yield [41]



$E_\gamma^{\max} = 8.4 \text{ MeV. } (E_e - E_{th}) = 1.02 \text{ MeV.}$

$\theta = 90^\circ$ (upper figure) and 135° (lower figure).

Sample: lead-208 enrichment 99.1%. Weight 49.3 g.

The figures near the peaks indicate the neutron energies in keV.

82 - Pb - 208

Resonance parameters

E _n lab (keV)		g _y Γ _{γo} Γ _n /Γ (eV)	GS or ES	J ^π		Γ _{γo} * (eV)		E _n ^{res} (keV)	
[27]	[4I]	[27]	[27]	[27]	[4I]	[27]	[4I]	[27]	[13d]
2,9		0,16	ES					3,0	
8,9		0,62							
9,9		0,12	GS					10,1	
15,9		0,17	GS	2 ⁺		0,06		16,2	17
24,9 **		0,40	GS					25,3	
30,2		0,30	GS	I ⁺		0,23		30,7	29
35,4		0,22	ES						
37,5		1,8	GS	2 ⁺		0,64		38,I	37
40,8		7,2	GS	I ⁻		4,8		41,4	4I
90,0		2,6	GS					91,3	
98,6		1,9	ES						
114		2,0		I ⁺		I,6		115	
129		5,4	GS					131	
138		3,6	ES						
156		0,98	GS					158	
166		0,90	GS					168	
182	18I	16,0	GS	I ⁺	I ⁺	I2,6	9,9	184	
257	254	26,2	GS	I ⁻	I ⁻	I7,5	16,4	260	
299	297	4,0	ES					0,9	
318	315	II,0	GS	I ⁺	I	7,7	I0,2	32I	
	334				2 ^{+,I⁺}			0,7	
	422								
	445				2 ^{+,I⁺}			I,5	
	457				I			2,2	
	484							I,6	
493	49I	3,2			I			2,0	498
547	538	I2,3	GS	I ⁻ (I ⁺)	I	8,2	I2,4	553	

Resonance parameters (continued)

E_n^{lab} (keV)	$g_{\gamma} \Gamma_{\gamma^*} / \Gamma$ (eV)	GS or ES	J^π			$\Gamma_{\gamma^*}^*$ (eV)		E_n^{res} (keV)
[27]	[4I]	[27]	[27]	[27]	[4I]	[27]	[4I]	[27]
558	55I	4,6				3,3		564
	602			I		8,0		
620	613	17,2	GS	I^+	I	14,6	19,7	627
659	65I	8,6		I^+	I	6,3	II,8	666
	699				I		4,4	
	737				I		3,5	
860	846	10,0	GS	I^+	I	7,8	10,I	869
	907				I		6,5	
	945				I		2,9	
	95I				I		3,5	
	996				I		5,8	

* The Γ_{γ^*} values were found in relation to the resonance of the ^{208}Pb (γ, n) γ^* reaction at energy 41 keV, for which the magnitude of Γ_{γ^*} was taken equal to 4.8 eV [27] and 4.2 eV [41].

** The data were taken from Ref. [7].

Radiation strength function

$$\langle \Gamma_{\gamma^*} / D \rangle = (4,0 \pm 3,6) \cdot 10^{-5} \quad [27].$$

Non-resonance process cross-section

$$0.8 \leq \sigma_{\text{NR}} \leq 1.2 \quad \text{mbarn/steradian} \quad [14].$$

Our evaluation of σ_{NR} is based on the assumption that the observed asymmetry in the peak at $E_{\text{lab}}^{\text{NR}} = 40.7$ keV (see Fig. on page 55) is due to interference of the direct and resonance mechanisms of the reaction.

82 - Pb - 208

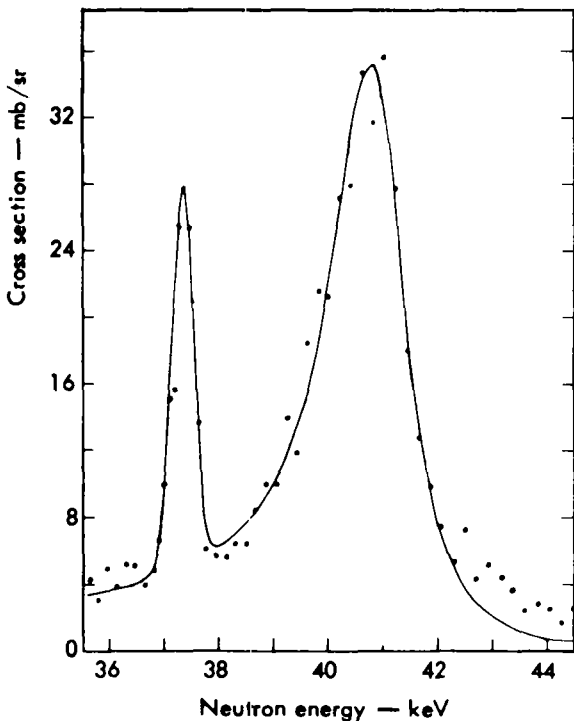
The following parameter values were obtained for the peak:

$$\Gamma_n = 1520 \text{ eV}, \\ 4.18 \leq \Gamma_{\gamma_0} \leq 6.44 \text{ eV}$$

Experimental conditions:

$$E_{\gamma}^{\max} = 9.0 \text{ MeV} \\ \theta = 135^\circ$$

Sample - natural lead



Doorway states [28]

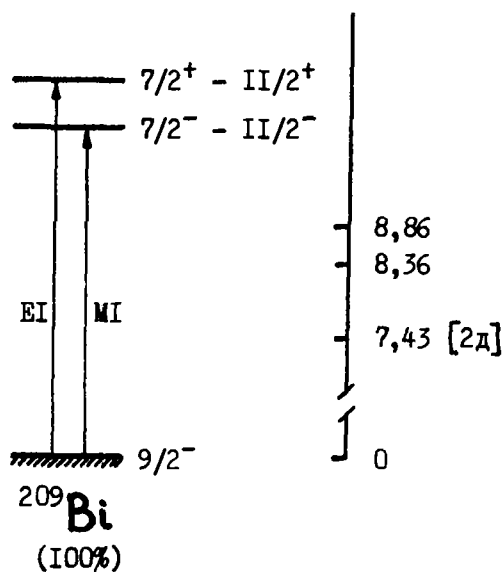
In the range of $E_n^{\text{lab}} = 30-860 \text{ keV}$, 7 MI resonances with $J^\pi = 1^+$ are found with a total radiation strength of 50.8 eV. These resonances may be associated with doorway states of type $I_p - I_h$ in a $i_{13/2}$ neutron shell or a $h_{11/2}$ proton shell.

BISMUTH-209

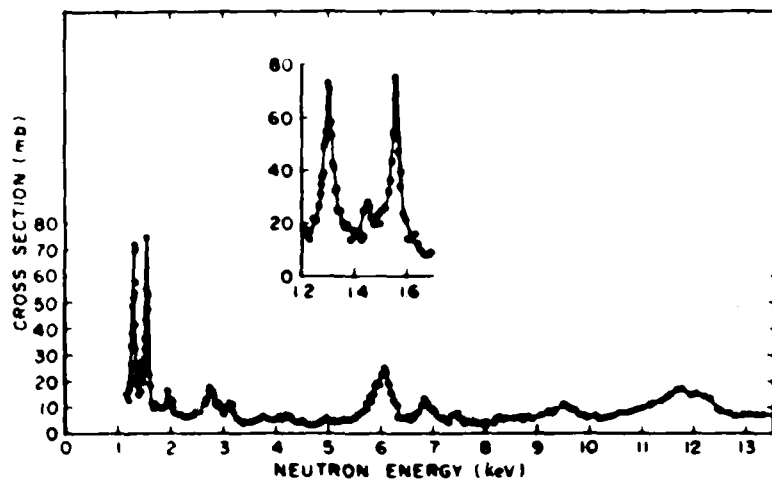
83 - Bi - 209

Level scheme [1d]

(I^{+}) $I430$ —————
 γ^{+} 930 —————
 5^{+} 0 208Bi



Differential cross-sections [3]



$$E_{\gamma}^{\max} = 11,0 \text{ MeV}$$

$$\theta = 135^\circ$$

Resolution = 15-30 nsec/m

A N N E X 1

SOME CHARACTERISTICS OF STABLE AND
LONG-LIVED ISOTOPES

Isotope	J^π	Abundance (%)	Neutron binding energy (MeV)	Decay of A - 1 nuclei
1-Hydrogen-2	I^+	0,0149	2,2247	stab.
2-Helium-3	$I/2^+$	0,000137		$2p$
2-Helium-4	0^+	99,999863	20,577	stab.
3-Lithium-6	I^+	7,42	5,663	$p + He^4$
3-Lithium-7	$3/2^-$	92,58	7,253	stab.
4-Beryllium-9	$3/2^-$	100	I,6651	2α ; $2,3 \cdot 10^{-16}$ sec
5-Boron-10	3^+	I9,61	8,4352	$p + 2\alpha$
5-Boron-11	$3/2^-$	80,39	II,4560	stab.
6-Carbon-12	0^+	98,893	I8,7219	β^+ ; 20,74 min
6-Carbon-13	$I/2^-$	I,107	4,9464	stab.
7-Nitrogen-14	I^+	99,6337	I0,5536	β^+ ; 9,965 min
7-Nitrogen-15	$I/2^-$	0,3663	I0,8337	stab.
8-Oxygen-16	0^+	99,759	I5,6694	β^+ ; I23 sec
8-Oxygen-17	$5/2^+$	0,0374	4,I424	stab.
8-Oxygen-18	0^+	0,2039	8,0468	stab.
9-Fluorine-19	$I/2^+$	100	I0,4307	β^+ ; I09,87 min

Isotope	J^π	Abundance (%)	Neutron binding energy (MeV)	Decay of A - 1 nuclei
I0-Neon-20	0 ⁺	90,92	I6,8655	β^+ ; I6,72 sec
I0-Neon-21	3/2 ⁺	0,257	6,76I2	stab.
I0-Neon-22	0 ⁺	8,82	I0,3656	stab.
II-Sodium-23	3/2 ⁺	I00	I2,4I78	β^+ ; 2,58 years
I2-Magnesium-24	0 ⁺	78,70	I6,5305	β^+ ; I2,I sec
I2-Magnesium-25	5/2 ⁺	I0,I3	7,33I9	stab.
I2-Magnesium-26	0 ⁺	II,I7	II,0937	stab.
I3-Aluminium-27	5/2 ⁺	I00	I3,058	β^+ ; 7,38·10 ⁵ years
I4-Silicon-28	0 ⁺	92,2I	I7,I774	β^+ ; 4,33 sec
I4-Silicon-29	1/2 ⁺	4,70	8,4738	stab.
I4-Silicon-30	0 ⁺	3,09	I0,6097	stab.
I5-Phosphorus-31	1/2 ⁺	I00	I2,3073	β^+ ; 2,497 min
I6-Sulphur-32	0 ⁺	95,0	I5,088	β^+ ; 2,6I sec
I6-Sulphur-33	3/2 ⁺	0,76	8,6434	stab.
I6-Sulphur-34	0 ⁺	4,22	II,4I49	stab.
I6-Sulphur-36	0 ⁺	0,0I36	9,8920	β^- ; 86,73 days
I7-Chlorine-35	3/2 ⁺	75,529	I2,6463	β^+ ; I,588 sec+ 32,40 min
I7-Chlorine-37	3/2 ⁺	24,47I	I0,3II3	β^- ; 3,08·10 ⁵ years
I8-Argon-36	0 ⁺	0,337	I5,2528	β^+ ; I,804 sec
I8-Argon-38	0 ⁺	0,063	II,8387	K ; 34,30 days
I8-Argon-40	0 ⁺	99,6	9,87I	β^- ; 269 years

Isotope	J^π	Abundance (%)	Neutron binding energy (MeV)	Decay of A - 1 nuclei
19-Potassium-39	$3/2^+$	93,I	13,085	β^+ ; 7,66 min
19-Potassium-40	4^-	0,0II8I	7,80053	stab.
19-Potassium-41	$3/2^+$	6,88	10,0959	β^- ; $1,27 \cdot 10^9$ years
20-Calcium-40	0^+	96,97	15,634	β^+ ; 0,873 sec
20-Calcium-42	0^+	0,64	II,4727	K ; $1,1 \cdot 10^5$ years
20-Calcium-43	$7/2^-$	0,I45	7,9326	stab.
20-Calcium-44	0^+	2,06	II,1363	stab.
20-Calcium-46	0^+	0,0033	10,404	β^- ; 161,5 days
20-Calcium-48	0^+	0,I85	9,95I	β^-
21-Scandium-45	$7/2^-$	100	II,32I	β^+ ; 3,92 hours + 2,44 days
22-Titanium-46	0^+	7,93	13,1968	β^+ ; 3,06 hours
22-Titanium-47	$5/2^-$	7,28	8,875I	stab.
22-Titanium-48	0^+	73,94	II,628I	stab.
22-Titanium-49	$7/2^-$	5,5I	8,I434	stab.
22-Titanium-50	0^+	5,34	10,9480	stab.
23-Vanadium-50	6^+	0,24	9,3323	K ; 334 days
23-Vanadium-51	$7/2^-$	99,76	II,0524	β^- ; $6 \cdot 10^{15}$ years
24-Chromium-50	0^+	4,3I	12,940	β^+ ; 4I,7 min
24-Chromium-52	0^+	83,76	12,0407	K ; 27,8 days
24-Chromium-53	$3/2^-$	9,55	7,9405	stab.
24-Chromium-54	0^+	2,38	9,7202	stab.
25-Manganese-55	$5/2^-$	100	10,224	K ; 3I3,5 days

Isotope	J^π	Abundance (%)	Neutron binding energy (MeV)	Decay of A - 1 nuclei
26-Iron-54	0^+	5,84	13,382	β^+ ; 8,5 min
26-Iron-56	0^+	91,68	11,2027	K; 2,6 years
26-Iron-57	$1/2^-$	2,17	7,6462	stab.
26-Iron-58	0^+	0,31	10,0430	stab.
27-Cobalt-59	$7/2^-$	100	10,4602	β^+ ; 71,3 days + 9,2 hours
28-Nickel-58	0^+	67,88	12,203	β^+ ; 36,5 hours
28-Nickel-60	0^+	26,23	11,3883	K; $7,5 \cdot 10^4$ years
28-Nickel-61	$3/2^-$	1,19	7,8195	stab.
28-Nickel-62	0^+	3,66	10,5966	stab.
28-Nickel-64	0^+	1,08	9,6596	β^- ; 91,6 years
29-Copper-63	$3/2^-$	69,09	10,854	β^+ ; 9,76 min
29-Copper-65	$3/2^-$	30,91	9,9047	β^\pm ; 12,88 hours
30-Zinc-64	0^+	48,89	11,8563	β^+ ; 38,4 hours
30-Zinc-66	0^+	27,81	11,052	β^+ ; 245 days
30-Zinc-67	$5/2^-$	4,11	7,0539	stab.
30-Zinc-68	0^+	18,57	10,1993	stab.
30-Zinc-70	0^+	0,62	9,2152	β^- ; 58,5 min + 13,9 hours
31-Gallium-69	$3/2^-$	60,4	10,310	β^+ ; 67,7 min
31-Gallium-71	$3/2^-$	39,6	9,3038	β^- ; 21,37 min
32-Germanium-70	0^+	20,52	11,533	β^+ ; 38,8 hours
32-Germanium-72	0^+	27,43	10,7493	K; 12,5 days
32-Germanium-73	$9/2^-$	7,76	6,7843	stab.

Isotope	J^π	Abundance (%)	Neutron binding energy (MeV)	Decay of A - 1 nuclei
32-Germanium-74	0^+	36,54	10,2009	stab.
32-Germanium-76	0^+	7,76	9,443	β^- ; 79 min + 49 sec
33-Arsenic-75	$3/2^-$	100	10,2426	β^\pm ; 17,74 hours
34-Selenium-74	0^+	0,87	12,071	β^+ ; 44 min + 7,I hours
34-Selenium-76	0^+	9,02	II,1613	K ; 120,4 days
34-Selenium-77	$1/2^-$	7,58	7,4185	stab.
34-Selenium-78	0^+	23,52	10,4970	stab.
34-Selenium-80	0^+	49,82	9,896	β^- ; $6,5 \cdot 10^4$ years + 3,9I min
34-Selenium-82	0^+	9,19	9,272	β^- ; 18,6 min + 62 min
35-Bromine-79	$3/2^-$	50,537	10,693	β^+ ; 6,5 min
35-Bromine-81	$3/2^-$	49,463	10,160	β^\pm ; 17,55 min + 4,37 hours
36-Krypton-78	0^+	0,354	II,98I	β^+ ; I,185 hours
36-Krypton-80	0^+	2,27	II,525	β^+ ; 34,92 hours + 55 sec
36-Krypton-82	0^+	II,56	10,980	K ; $2,13 \cdot 10^5$ years + I3 sec
36-Krypton-83	$9/2^+$	II,55	7,467	stab.
36-Krypton-84	0^+	56,90	10,705	stab.
36-Krypton-86	0^+	I7,37	9,860	β^- ; 10,76 years + 4,5 hours
37-Rubidium-85	$5/2^-$	72,15	10,478	β^+ ; 33 days + 20 min
37-Rubidium-87	$3/2^-$	27,85	9,926	β^- ; 18,66 days + I,02 min

Isotope	J^π	Abundance (%)	Neutron binding energy (MeV)	Decay of A - 1 nuclei
38-Strontium-84	0 ⁺	0,56	I2,0I3	β^+ ; 32,9 hours
38-Strontium-86	0 ⁺	9,86	II,485	K ; 63,9 days + 70 min
38-Strontium-87	9/2 ⁺	7,02	8,4283	stab.
38-Strontium-88	0 ⁺	82,56	II,II32	III; 2,80 hours
39-Yttrium-89	I/2 ⁻	100	II,468	β^+ ; 105 days
40-Zirconium-90	0 ⁺	5I,46	II,983	β^+ ; 78,4 hours + 4,I8 min
40-Zirconium-91	5/2 ⁺	II,23	7,2026	stab.
40-Zirconium-92	0 ⁺	I7,II	8,635I	stab.
40-Zirconium-94	0 ⁺	I7,40	8,I9I	β^- ; 9,5·10 ⁵ years
40-Zirconium-96	0 ⁺	2,80	7,832	β^- ; 65,2 days
41-Niobium-93	9/2 ⁺	100	8,826	K ; 10,I6 days
42-Molybdenum-92	0 ⁺	I5,84	I2,692	β^+ ; 15,7 min + 64 sec
42-Molybdenum-94	0 ⁺	9,04	9,6722	K ; 100 years
42-Molybdenum-95	5/2 ⁺	I5,72	7,375I	stab.
42-Molybdenum-96	0 ⁺	I6,53	9,I542	stab.
42-Molybdenum-97	5/2 ⁺	9,46	6,8I6I	stab.
42-Molybdenum-98	0 ⁺	23,78	8,6424	stab.
42-Molybdenum-100	0 ⁺	9,63	8,30I	β^- ; 67 hours
44-Ruthenium-96	0 ⁺	5,5I	I0,694	β^+ ; I,65 hours
44-Ruthenium-98	0 ⁺	I,87	I0,250	K ; 2,88 days
44-Ruthenium-99	5/2 ⁺	I2,72	7,468	stab.
44-Ruthenium-100	0 ⁺	I2,62	9,6735	stab.
44-Ruthenium-101	5/2 ⁺	I7,07	6,805	stab.
44-Ruthenium-102	0 ⁺	3I,6I	9,2I6I	stab.

Isotope	J^π	Abundance (%)	Neutron binding energy (MeV)	Decay of A - 1 nuclei
44-Ruthenium-104	0^+	18,58	8,912	β^- ; 39,4 days
45-Rhodium-103	$1/2^-$	100	9,310	β^\pm ; 210 days + 2,5 years
46-Palladium-102	0^+	0,96	10,587	K ; 8,5 hours
46-Palladium-104	0^+	10,97	10,020	K ; 17 days
46-Palladium-105	$5/2^+$	22,23	7,073	stab.
46-Palladium-106	0^+	27,33	9,561	stab.
46-Palladium-108	0^+	26,71	9,225	β^- ; $7 \cdot 10^6$ years + 21,3 sec
46-Palladium-110	0^+	11,81	8,806	β^- ; 13,45 hours + 4,69 min
47-Silver-107	$1/2^-$	51,35	9,551	β^+ ; 2,4 min + 8,3 days
47-Silver-109	$1/2^-$	48,65	9,188	β^- ; 2,42 min + >5 years
48-Cadmium-106	0^+	1,24	10,920	β^+ ; 54,7 min
48-Cadmium-108	0^+	0,871	10,329	K ; 6,7 hours
48-Cadmium-110	0^+	12,32	9,879	K ; 470 days
48-Cadmium-111	$1/2^+$	12,67	6,9768	stab.
48-Cadmium-112	0^+	24,15	9,397	stab.
48-Cadmium-113	$1/2^+$	12,24	6,5398	stab.
48-Cadmium-114	0^+	28,93	9,041	stab.
48-Cadmium-116	0^+	7,61	8,696	β^- ; 2,2 days + 43 days
49-Indium-113	$9/2^+$	4,28	9,424	β^\pm ; 11 min + 22 min
49-Indium-115	$9/2^+$	95,72	9,029	β^\pm ; 72 sec + 50 days

Isotope	J^π	Abundance (%)	Neutron binding energy (MeV)	Decay of A - 1 nuclei
50-Tin-112	0 ⁺	0,96	10,802	K ; 35 min
50-Tin-114	0 ⁺	0,66	10,320	K ; II 8 days + 27 min
50-Tin-115	1/2 ⁺	0,35	7,534	stab.
50-Tin-116	0 ⁺	14,3	9,566	stab.
50-Tin-117	1/2 ⁺	7,61	6,9425	stab.
50-Tin-118	0 ⁺	24,03	9,3273	III; I 4 days
50-Tin-119	1/2 ⁺	8,58	6,485	stab.
50-Tin-120	0 ⁺	32,85	9,1044	III; 250 days
50-Tin-122	0 ⁺	4,72	8,8047	β^- ; 28,2 hours + 5 years
50-Tin-124	0 ⁺	5,94	8,493	β^- ; 40 min I 25 days
51-Antimony-121	5/2 ⁺	57,25	9,248	β^+ ; I,62 min + 5,8 days
51-Antimony-123	7/2 ⁺	42,75	8,9653	β^- ; 2,75 days + 3,3 min
52-Tellurium-120	0 ⁺	0,089	10,286	β^+ ; I 5,9 hours + 4,5 days
52-Tellurium-122	0 ⁺	2,46	9,79	K ; I 7 days + I 54 days
52-Tellurium-123	1/2 ⁺	0,89	6,9299	stab.
52-Tellurium-124	0 ⁺	4,74	9,4238	III; I 04 days
52-Tellurium-125	1/2 ⁺	7,03	6,5849	stab.
52-Tellurium-126	0 ⁺	I 8,72	9,1093	III; 58 days
52-Tellurium-128	0 ⁺	31,75	8,772	β^- ; 9,35 hours + I 05 days
52-Tellurium-130	0 ⁺	34,27	8,413	β^- ; 74 min + 41 days
53-Iodine-127	5/2 ⁺	100	9,139	β^\pm ; I 3,I days + 26 hours

Isotope	J^π	Abundance (%)	Neutron binding energy (MeV)	Decay of A - 1 nuclei
54-Xenon-124	0^+	0,096	10,23	β^+ ; 7,85 hours
54-Xenon-126	0^+	0,090	10,09	K ; 17 hours
54-Xenon-128	0^+	1,919	9,614	K ; 36,41 days
54-Xenon-129	$1/2^+$	26,44	6,905	stab.
54-Xenon-130	0^+	4,08	9,258	III; 89 days
54-Xenon-131	$3/2^+$	21,18	6,6056	stab.
54-Xenon-132	0^+	26,89	8,9361	III; 12 days
54-Xenon-134	0^+	10,44	8,535	β^- ; 5,65 days + 2,2 days
54-Xenon-136	0^+	8,87	7,992	β^- ; 9,13 hours + 15,8 min
55-Caesium-133	$7/2^+$	100	8,979	K ; 6,48 days
56-Barium-130	0^+	0,101	10,22	β^+ ; 2,61 hours + 2,10 hours
56-Barium-132	0^+	0,097	9,803	K ; II,52 days
56-Barium-134	0^+	2,42	9,4644	K ; 7,5 years + 38,9 hours
56-Barium-135	$3/2^+$	6,59	6,9752	stab.
56-Barium-136	0^+	7,81	9,1071	III; 28,7 hours
56-Barium-137	$3/2^+$	II,32	6,9021	stab.
56-Barium-138	0^+	71,66	8,6115	III; 2,57 min
57-Lanthanum-138	5	0,089	7,32	K ; $6 \cdot 10^4$ years
57-Lanthanum-139	$7/2^+$	99,911	8,7778	K ; $1,1 \cdot 10^{11}$ years
58-Cerium-136	0^+	0,193	10,01	K ; 18 hours
58-Cerium-138	0^+	0,25	9,57	K ; 9 hour + 34,4 hours
58-Cerium-140	0^+	88,48	9,203	K ; 140 days + 60 sec
58-Cerium-142	0^+	II,07	7,160	β^- ; 32,5 days

Isotope	J^π	Abundance (%)	Neutron binding energy (MeV)	Decay of A - 1 nuclei
59-Praseodymium-141	$5/2^+$	100	9,397	β^+ ; 3,4 min
60-Neodymium-142	0^+	27,II	9,813	K ; 2,42 hours + 63,9 sec
60-Neodymium-143	$7/2^-$	I2,I7	6,I255	stab.
60-Neodymium-144	0^+	23,85	7,8I74	stab.
60-Neodymium-145	$7/2^-$	8,30	5,7604	α ; $2,4 \cdot 10^{15}$ years
60-Neodymium-146	0^+	I7,2	7,5654	stab.
60-Neodymium-148	0^+	5,73	7,324I	β^- ; II,06 days
60-Neodymium-150	0^+	5,62	7,357	β^- ; I8 hours
62-Samarium-144	0^+	3,09	I0,554	β^+ ; 8,6 min
62-Samarium-147	$7/2^-$	I4,97	6,373	α ; $5 \cdot 10^7$ years
62-Samarium-148	0^+	II,24	8,I407	α ; $1,05 \cdot 10^{10}$ years
62-Samarium-149	$7/2^-$	I3,83	5,873I	stab.
62-Samarium-150	0^+	7,44	7,986I	α ; $4 \cdot 10^{14}$ years
62-Samarium-152	0^+	26,72	8,2668	β^- ; 93 years
62-Samarium-154	0^+	22,7I	7,978	β^- ; 47 hours
63-Europium-151	$5/2^+$	47,82	7,982	K ; I4 hours
63-Europium-153	$5/2^+$	52,I8	8,555	β^- ; I2,7 years + 9,I hours
64-Gadolinium-152	0^+	0,205	8,597	K ; I20 days
64-Gadolinium-154	0^+	2,23	8,657	K ; 200 days
64-Gadolinium-155	$3/2^-$	I5,I	6,446	stab.
64-Gadolinium-156	0^+	20,6	8,53I2	stab.
64-Gadolinium-157	$3/2^-$	I5,7	6,3682	stab.
64-Gadolinium-158	0^+	24,50	7,9307	stab.
64-Gadolinium-160	0^+	2I,6	7,453	β^- ; I8 hours

Isotope	J^π	Abundance (%)	Neutron binding energy (MeV)	Decay of A - 1 nuclei
65-Terbium-159	$3/2^+$	100	8,136	K ; 1200 years
66-Dysprosium-156	0^+	0,0524	9,442	β^+ ; 10 hours
66-Dysprosium-158	0^+	0,0902	9,061	K ; 8,2 hours
66-Dysprosium-160	0^+	2,294	8,582	K ; 144,4 days
66-Dysprosium-161	$5/2^+$	18,9	6,45II	stab.
66-Dysprosium-162	0^+	25,53	8,1949	stab.
66-Dysprosium-163	$5/2^-$	24,97	6,27I7	stab.
66-Dysprosium-164	0^+	28,18	7,6547	stab.
67-Holmium-165	$7/2^-$	100	7,989	β^- ; 26 min
68-Erbium-162	0^+	0,136	9,2I	K ; 3 hours
68-Erbium-164	0^+	1,56	8,856	K ; 75 min
68-Erbium-166	0^+	33,4I	8,474	K ; 10,5 hours
68-Erbium-167	$7/2^+$	22,94	6,4363	stab.
68-Erbium-168	0^+	27,07	7,77I4	stab.
68-Erbium-170	0^+	14,88	7,263I	β^- ; 9,6 days
69-Thulium-169	$1/2^+$	100	8,06	K ; 85 days
70-Ytterbium-168	0^+	0,135	9,055	K ; 17,7 min
70-Ytterbium-170	0^+	3,14	8,469	K ; 30,6 days
70-Ytterbium-171	$1/2^-$	14,40	6,6172	stab.
70-Ytterbium-172	0^+	21,90	8,0239	stab.
70-Ytterbium-173	$5/2^-$	16,2	6,3677	stab.
70-Ytterbium-174	0^+	31,6	7,469I	stab.
70-Ytterbium-176	0^+	12,60	6,876	β^- ; 4,2 days

Isotope	J^π	Abundance (%)	Neutron binding energy (MeV)	Decay of A - 1 nuclei
71-Lutetium-175	7/2 ⁺	97,4I	7,659	K ; I40 + I300 days
71-Lutetium-176	7 ⁻	2,59	6,2932	stab.
72-Hafnium-174	0 ⁺	0,18	8,59	K ; 24 hours
72-Hafnium-176	0 ⁺	5,20	8,089	K ; 70 days
72-Hafnium-177	7/2 ⁻	I8,50	6,3808	stab.
72-Hafnium-178	0 ⁺	27,I4	7,626I	stab.
72-Hafnium-179	9/2 ⁺	I3,75	6,0995	stab.
72-Hafnium-180	0 ⁺	35,24	7,3876	stab.
73-Tantaleum-180	8	0,0II7	6,580	K ; 600 days
73-Tantaleum-181	7/2 ⁺	99,9883	7,644	K ; I,7 · 10 ¹³ years + 8,15 hours
74-Tungsten-180	0 ⁺	0,I35	8,49	
74-Tungsten-182	0 ⁺	26,4I	8,054	K ; I20 days
74-Tungsten-183	I/2 ⁻	I4,40	6,I9I4	stab.
74-Tungsten-184	0 ⁺	30,64	7,4III	stab.
74-Tungsten-186	0 ⁺	28,4I	7,202	β^- ; 75,8 days
75-Rhenium-185	5/2 ⁺	37,07	7,79	K ; 38 + I65 days
75-Rhenium-187	5/2 ⁺	62,93	7,37I4	β^- ; 88,9 hours
76-Osmium-186	0 ⁺	I,59	8,2705	K ; 93,6 days
76-Osmium-187	I/2 ⁻	I,64	6,297	stab.
76-Osmium-188	0 ⁺	I3,3	7,989	III; 39 hours
76-Osmium-189	3/2 ⁻	I6,I	5,9233	stab.
76-Osmium-190	0 ⁺	26,4	7,793I	stab.
76-Osmium-192	0 ⁺	4I,0	7,559	β^- ; I4,6 days + I4 hours

Isotope	J^π	Abundance (%)	Neutron binding energy (MeV)	Decay of A - 1 nuclei
77-Iridium-191	$3/2^+$	37,3	8,12	K; 12,3 days + 3,2 hours
77-Iridium-193	$3/2^+$	62,7	7,772	β^- ; 74,4 days + 1,45 min
78-Platinum-190	0^+	0,0127	8,81	K ; 10,5 hours
78-Platinum-192	0^+	0,78	8,656	K ; 3 days
78-Platinum-194	0^+	32,9	8,367	K ; 500 years
78-Platinum-195	$1/2^-$	33,8	6,124	stab.
78-Platinum-196	0^+	25,3	7,9209	stab.
78-Platinum-198	0^+	7,21	7,563	β^- ; 18 hours + 80 min
79-Gold-197	$3/2^+$	100	8,08	K ; 6,15 days
80-Mercury-196	0^+	0,14	8,75	K ; 9,5 + 40 hours
80-Mercury-198	0^+	10,02	8,30	K ; 65 + 24 hours
80-Mercury-199	$1/2^-$	16,84	6,6483	stab.
80-Mercury-200	0^+	23,13	8,0287	stab.
80-Mercury-201	$3/2^-$	13,22	6,2254	stab.
80-Mercury-202	0^+	29,80	7,7566	stab.
80-Mercury-204	0^+	6,85	7,491	β^- ; 46,9 hours
81-Thallium-203	$1/2^+$	29,50	7,72	K ; 12 days
81-Thallium-205	$1/2^+$	70,50	7,5414	β^- ; 3,78 years
82-Lead-204	0^+	1,37	8,401	K ; 52,1 hours
82-Lead-206	0^+	25,0	8,081	K ; $2,4 \cdot 10^7$ years
82-Lead-207	$1/2^-$	21,2	6,7409	stab.
82-Lead-208	0^+	52,4	7,3682	stab.

Isotope	Γ^{∞}	Abundance (%)	Neutron binding energy (MeV)	Decay of A - 1 nuclei
83-Bismuth-209	$9/2^-$	100	7,453	κ ; $3 \cdot 10^4$ years
80-Thorium-232	0^+	100	6,434	β^- ; 25,64 hours
92-Uranium-234	0^+	0,0056	6,8408	α ; $16,2 \cdot 10^4$ years
92-Uranium-235	$7/2^-$	0,7205	5,306	α ; $2,5 \cdot 10^5$ years
92-Uranium-238	0^+	99,2739	6,1436	β^- ; 6,75 days

BIBLIOGRAPHIC INDEX OF WORK ON PHOTONEUTRON REACTIONS NEAR THE THRESHOLD

Nucleus	Quantity	Type of data	E PRIM min	E PRIM max	E SEC min	E SEC max	NT LAB	Author(s)	Source	Year	Comments
HE 004	GN+NG	GRPH	22+7	31+7	10+5	80+6	EJ	LRL BERMAN+	MASH 1136 8?	969	
BE 009	GN DIF SIG	GRPH	35+6		1+3	40+4	EJ	LRL BERMAN+	PR 163 95A	967	TOF; SC+H(1) 135 DEG; PT TGT;
BE 009	RES PARAH	TBL	35+6		1+3	40+4	EJ	LRL BERMAN+	PR 163 95B	967	NG=1.8 EV;
B 010	GN DIF SIG	GRPH	10+7		10+4	91+5	ED	LRL VAN HEMERT	UCRL 50501	965	
F 019	GN DIF SIG	GRPH	11+7		10+4	10+6	ED	LRL VAN HEMERT	UCRL 50501	968	
F 019	GN DIF SIG	GRPH	11+7		20+4	80+5	EJ	LRL BAGLAN+	PR 3 C672	271	TOF; SCU5GG; 3.5 NS/M; 135 DEG;
F 019	RES PARAH	TBL	12+7		10+5		EJ	LRL BAGLAN+	PR 3 C672	271	
MG 024	GN DIF SIG	GRPH	16+7	19+7	10+4	22+6	ED	LRL VAN HEMERT	UCRL 50501	968	
MG 024	GN DIF SIG	GRPH	20+7		10+4	20+6	EJ	LRL BAGLAN+	PR 3 C672	271	TOF; SCU5GG; 2.3 NS/M; 135 DEG;
MG 024	RES PARAH	NDG					EA	LRL BOWMAN+	MASH 1127 96	469	
MG 024	RES PARAH	TBL	20+7		22+4	20+6	EJ	LRL BAGLAN+	PR 3 C672	271	
MG 024	ANALG STS	TEXT					ED	LRL VAN HEMERT	UCRL 50501	968	
MG 025	GN DIF SIG	GRPH	83+6	11+7	10+4	14+6	ED	LRL VAN HEMERT	UCRL 50501	968	
MG 025	GN DIF SIG	GRPH	11+7		30+4	20+6	EJ	LRL BERMAN+	PRL 24 319	270	TOF; 135 DEG; Y TGT;
MG 025	GN DIF SIG	GRPH	11+7		25+4	20+6	ED	LRL BAGLAN	UCRL 50902	870	
MG 025	GN DIF SIG	GRPH	11+7		25+4	20+6	EJ	LRL BAGLAN+	PR 3 C672	271	TOF; SCU5GG; 1.6 NS/M; 135 DEG;
MG 025	RES PARAH	TEXT	11+7		30+4	20+6	EJ	LRL BERMAN+	PRL 24 319	270	
MG 025	RES PARAH	TBL	83+6	11+7	41+4	12+6	ED	LRL BAGLAN	UCRL 50902	870	
MG 025	RES PARAH	TBL	83+6	11+7	41+4	18+6	EJ	LRL BAGLAN+	PR 3 C672	271	
MG 025	GN NOR RESN	NDG					EA	LRL BOWMAN+	MASH 1127 96	469	
MG 025	ANALG STS	NDG					EA	LRL BOWMAN+	MASH 1127 96	469	
MG 025	ANALG STS	TEXT	11+7		30+4	20+6	EJ	LRL BERMAN+	PRL 24 319	270	
MG 025	ANALG STS	TEXT	11+7		40+5		ED	LRL BAGLAN	UCRL 50902	870	
MG 025	ANALG STS	TEXT	11+7		44+5	12+6	EJ	LRL BAGLAN+	PR 3 C672	271	
MG 025	ANALG STS	TEXT					EJ	LLL BERMAN+	PR 6 C2295	072	
MG 026	GN DIF SIG	SPFH	11+7	13+7	10+4	15+6	ED	LRL VAN HEMERT	UCRL 50501	968	
MG 026	GN DIF SIG	GRPH	13+7		10+4	15+6	EJ	LRL BERMAN+	PRL 23 386	869	TOF; 135 DEG; FOR ASTROPHYS PROBLEMS;
MG 026	GN DIF SIG	GRPH	13+7		10+4	15+6	EJ	LRL BAGLAN+	PR 3 C672	271	TOF; SCU5GG; 2.3 NS/M; 135 DEG;
MG 026	RES PARAH	NDG					EA	LRL BOWMAN+	MASH 1127 96	469	
MG 026	RES PARAH	TBL	13+7		54+4	11+6	EJ	LRL BAGLAN+	PR 3 C672	271	
MG 026	STRNG FNC GO	TBL					EA	LRL BAGLAN+	MCSAC 33 105	070	
MG 026	STRNG FNC GO	TEL					EJ	LRL BAGLAN+	PR 3 C672	271	$S(GO)=(3.1+-2.0)E-5$
SI 028	GN DIF SIG	GRPH	18+7		10+4	70+5	ED	LRL VAN HEMERT	UCRL 50501	965	
SI 029	GN YIELD	NDG					EA	ANL JACKSON+	MCSAC 42 24	N71	
SI 029	GN YIELD	GRPH			10+4	14+6	EA	ANL JACKSON+	USNDG 1 13	572	
SI 029	GN YIELD	GRPH	10+7		3+5	13+6	EJ	ANL JACKSON+	PRL 29 379	872	TOF; SC+H(NN); 90 DEG;
SI 029	DOORWAY STS	TEXT					EA	ANL JACKSON+	USNDG 1 13	572	
SI 029	DOORWAY STS	TEXT					EJ	ANL JACKSON+	PRL 29 379	872	DOORWAY STATE NEAR 750 KEV;
SI 029	GN NOR RESN	TEXT					EA	ANL JACKSON+	USNDG 1 13	572	
SI 029	ANALG STS	TEXT					EA	ANL JACKSON+	MCSAC 42 24	N71	
F 031	GN DIF SIG	GRPH	14+7		10+4	13+6	ED	LRL VAN HEMERT	UCRL 50501	968	
F 031	RES PARAH	TBL	14+7		10+5	94+5	EJ	LRL BAGLAN+	PR 3 C672	271	
S 032	GN DIF SIG	GRPH	17+7		10+4	10+6	ED	LRL VAN HEMERT	UCRL 50501	968	
AR 040	GN DIF SIG	GRPH	13+7		4+5	25+6	EJ	OTC LOKAN+	PRL 28 1526	672	TOF; SC+H(NN); 90 DEG; TA TGT;
CA 040	GN DIF SIG	GRPH	17+7		10+4	10+6	ED	LRL VAN HEMERT	UCRL 50501	968	
CR 052	GN DIF SIG	GRPH	14+7		60+4	10+6	ED	LRL BAGLAN	UCRL 50902	870	
CR 052	GN DIF SIG	GRPH	14+7		60+4	10+6	EJ	LRL BAGLAN+	PR 3 C672	271	TOF; SCU5GG; 1.1 NS/M; 135 DEG;
CR 052	RES PARAH	TBL	12+7	14+7	68+4	39+5	ED	LRL BAGLAN	UCRL 50902	870	
CR 052	RES PARAH	TBL	12+7	14+7	68+4	39+5	EJ	LRL BAGLAN+	PR 3 C672	271	
CR 052	STRNG FNC GO	TBL					ED	LRL BAGLAN	UCRL 50902	870	
CR 053	STRNG FNC GO	TBL					EJ	LRL BAGLAN+	PR 3 C672	271	$S(GO)=(1.6+-0.8)E-5$
CR 052	ANALG STS	NDG					EA	LRL BOWMAN+	MASH 1127 96	469	
CR 052	ANALG STS	NDG					ED	LRL BAGLAN	UCRL 50902	870	
CR 052	ANALG STS	NDG					EA	LRL BAGLAN+	MCSAC 33 106	070	
CR 052	ANALG STS	TEXT	14+7		60+5	10+6	EJ	LRL BAGLAN+	PR 3 C672	271	

Nucleus	Quantity	Type	E PRIM		E SEC		NT	LAB	Author(s)	Source	Year	Comments
		of data	min	max	min	max						
CR 053	GN YIELD	GRPH			20+4	52+5	EA	ANL	JACKSON	NCSAC 33 9	070	
CR 053	GN YIELD	GRPH	91+6		21+4	52+5	EJ	ANL	JACKSON+	PR 4 C1314	071	TOF; LIGLASS; 1 NS/M; 135 DEG;
CR 053	GN DIF SIG	GRPH			20+4	20+5	EA	LRL	BAGLAN+	NCSAC 31 100	570	
CR 053	GN DIF SIG	GRPH	12+7		20+4	16+6	ED	LRL	BAGLAN	UCRL 50902	870	
CR 053	GN DIF SIG	GRPH	12+7		20+4	16+6	EJ	LRL	BAGLAN+	PR 3 C672	271	TOF; SCU5GG; 1.1 NS/M; 135 DEG;
CR 053	GN DIF SIG	GRPH	12+7		20+4	16+6	EJ	LRL	BAGLAN+	PR 3 C2475	671	TOF; SCU5GG; 135 DEG;
CR 053	RES PARAM	NDG			EA	LRL	BOWMAN+	MASH	1127 96	469		
CR 053	RES PARAM	TBL	92+6	12+7	21+4	52+5	ED	LRL	BAGLAN	UCRL 50902	870	
CR 053	RES PARAM	TBL			21+4	37+5	EA	ANL	JACKSON	NCSAC 33 9	070	
CR 053	RES PARAM	TBL	92+6	12+7	21+4	55+5	EJ	LRL	BAGLAN+	PR 3 C672	271	
CR 053	RES PARAM	TBL			48+4	37+5	EJ	ANL	JACKSON+	PR 4 C1314	071	
CR 053	STRNG FNC GO	TBL			ED	LRL	BAGLAN	UCRL 50902	870			
CR 053	STRNG FNC GO	TBL			EA	LRL	BAGLAN+	NCSAC 33 106	070			
CR 053	DOORWAY STS	TEXT			20+4	20+5	EA	LRL	BAGLAN+	NCSAC 31 100	570	
CR 053	DOORWAY STS	TEXT	12+7		50+4	60+5	EJ	LRL	BAGLAN+	PR 3 C672	271	
CR 053	DOORWAY STS	TEXT	12+7		20+4	16+6	EJ	LRL	BAGLAN+	PR 3 C2475	671	
FE 057	GN YIELD	GRPH	12+7		1+3	10+4	EC	FEI	ABRAMOV+	71 KIEV	571	TOF; SC+B10; 30 NS/M; 75 DEG; AL TGT;
FE 057	GN DIF SIG	GRPH	13+7		1+3	12+4	EJ	LRL	BERMAN+	PRL 17 761	066	TOF; SC+B10; 15-30 NS/M; 135 DEG;
FE 057	GN DIF SIG	GRPH	13+7		1+3	70+4	EJ	LRL	BOWMAN+	PR 163 951	N67	TOF; SC+B10; 15 NS/M; 135 DEG; AL TGT;
FE 056	GN DIF SIG	NDG			EA	GA	SUND+	NCSAC 31 68	570			
FE 056	GN DIF SIG	GRPH	13+7		60+4	10+6	ED	LRL	BAGLAN	UCPL 50902	870	
FE 056	GN DIF SIG	GRPH			50+4	10+6	EA	LRL	BAGLAN	NCSAC 33 106	070	
FE 056	GN DIF SIG	GRPH	13+7		60+4	10+6	EJ	LRL	BAGLAN+	PR 3 C672	271	TOF; SCU5GG; 1.1 NS/M; 135 DEG;
FE 056	RES PARAM	TEL	12+7	13+7	19+3	98+3	EJ	LRL	BOWMAN+	PR 163 951	N67	
FE 056	RES PARAM	TEL	11+7	13+7	83+4	71+5	ED	LRL	BAGLAN	UCRL 50902	870	
FE 056	RES PARAM	TEL	11+7	13+7	83+4	71+5	EJ	LRL	BAGLAN+	PR 3 C672	271	
FE 056	STRNG FNC GO	TEL			ED	LRL	BAGLAN	UCRL 50902	870			
FE 056	ANALG STS	NDG			EA	LRL	BOWMAN+	MASH	1127 96	469		
FE 056	ANALG STS	NDG			ED	LRL	BAGLAN	UCRL 50902	870			
FE 056	ANALG STS	TEXT			30+5	75+5	EA	LRL	BAGLAN+	NCSAC 33 106	070	
FE 056	ANALG STS	TFXT	13+7		30+5	75+5	EJ	LRL	BAGLAN+	PR 3 C672	271	
FE 057	GN YIELD	GRPH	85+6		25+4	61+5	EJ	ANL	JACKSON+	PR 4 C1314	071	TOF; LIGLASS; 1 NS/M; 135 DEG;
FE 057	GN YIELD	GRPH	87+6		20+5	80+5	EA	ANL	JACKSON	NCSAC 42 23	N71	
FE 057	GN YIELD	GRPH	85+6		32+4	61+5	EJ	ANL	JACKSON+	PRL 27 1654	D71	TOF; LIGLASS; 90 DEG;
FE 057	GN YIELD	GRPH	87+6		20+5	80+5	EJ	ANL	JACKSON+	PRL 27 1654	D71	TOF; SCH(NN); 90 DEG;
FE 057	GN DIF SIG	GRPH	12+7		20+4	16+6	ED	LRL	BAGLAN	UCRL 50902	870	
FE 057	GN DIF SIG	GRPH	12+7		20+4	16+6	EJ	LRL	BAGLAN+	PR 3 C672	271	TOF; SCU5GG; 1.1 NS/M; 135 DEG;
FE 057	GN DIF SIG	GRPH	12+7		20+4	16+6	EJ	LRL	BAGLAN+	PR 3 C2475	671	TOF;
FE 057	RES PARAM	NDG			EA	LRL	BOWMAN+	MASH	1127 96	469		
FE 057	RES PARAM	TEL	86+6	12+7	26+4	39+5	ED	LRL	BAGLAN	UCRL 50902	870	
FE 057	RES PARAM	TEL	86+6	12+7	26+4	39+5	EJ	LRL	BAGLAN+	PR 3 C672	271	
FE 057	RES PARAM	TEL			27+4	28+5	EJ	ANL	JACKSON+	PR 4 C1314	071	
FE 057	RES PARAM	TEL			26+4	63+5	EA	ANL	JACKSON+	NCSAC 42 23	N71	
FE 057	STRNG FNC GO	TEL			ED	LRL	BAGLAN	UCRL 50902	870			
FE 057	STRNG FNC GO	TEL			EA	LRL	BAGLAN+	NCSAC 33 106	070			
FE 057	STRNG FNC GO	TEL			EJ	LRL	BAGLAN+	PR 3 C672	271	$S(G0) = (1.1 \pm 0.6) \times 10^{-5}$		
FE 057	DOORWAY STS	NDG			ED	LRL	BAGLAN+	UCRL 50902	870			
FE 057	DOORWAY STS	TEXT			EA	LRL	BAGLAN+	NCSAC 33 106	070			
FE 057	DOORWAY STS	TEXT	12+7		60+4	60+5	EJ	LRL	BAGLAN+	PR 3 C672	271	NO STRONG CORRELATION
FE 057	DOORWAY STS	TEXT	12+7		20+4	16+6	EJ	LRL	BAGLAN+	PR 3 C2475	671	DOORWAY STS NEAR 50 AND 250 KEV
FE 057	DOORWAY STS	TEXT			EA	ANL	JACKSON+	NCSAC 42 23	N71			
FE 057	DOORWAY STS	TEXT			EJ	ANL	JACKSON+	PRL 27 1654	D71	INTERMEDIATE STRUCTURE IN P-WAVE RESONANCES;		
FE 057	GN NON RESN	TEXT			22+4	28+4	ED	LRL	BAGLAN	UCRL 50902	870	
NI 061	GN YIELD	GRPH	89+6		11+4	25+5	EJ	ANL	JACKSON+	PR 4 C1314	071	TOF; LIGLASS; 1 NS/M; 90 DEG;
NI 061	RES PARAM	TEL			11+4	19+5	EJ	ANL	JACKSON+	PR 4 C1314	071	

Nucleus	Quantity	Type	E PRIM		E SEC		NT	LAB	Author(s)	Source	Year	Comments		
		of data	min	max	min	max								
ZR 091	GN YIELD	NDG			EA	ANL	TOOHEY+	USNDC	1 15	572				
SN 117	GN DIF SIG	GRPH	92+6		EJ	WRL	WINHOLD+	PL	7 607	870	TOF; SC+H(NN); 3 NS/M; 130 DEG;			
SN 119	GN YIELD	NDG			EA	ANL	STRAIT+	NCSAC	42 26	N71				
SN 119	GN DIF SIG	GRPH	92+6		EJ	WRL	WINHOLD+	PL	7 607	870	TOF; SC+H(NN); 3 NS/M; 130 DEG;			
PB	GN YIELD	GRPH	82+6	30+4	50+5	EJ	MIT	BERTOZZI+	PL	6 108	863	TOF; SC+AG(NG); 12 NS/M; 77 DEG; 0		
PB	GN YIELD	GRPH	74+6	12+5	40+5	EA	ANL	JACKSON	NCSAC	31 10	57			
PB	GN DIF SIG	GRPH	9+6	36+4	44+4	ED	LRL	BAGLAN	UCRL	50902	87			
PB	GN DIF SIG	GRPH	98+6	35+5	11+6	EJ	LRL	BOWMAN+	PRL	25 1302	N70	TOF; SC+H(NN); 135 DEG;		
PB 206	GN YIELD	GRPH	83+6	10+7	1 +3	50+4	EJ	LRL	BOWMAN+	PR	178 1827	269	TOF; SC+B10; PULSE-SHAPE DISCRIM;	
PB 206	GN DIF SIG	GRPH	10+7	6 +3	10+6	ED	LRL	BAGLAN	UCRL	50902	87			
PB 206	GN DIF SIG	GRPH	10+7	6 +3	10+6	EJ	LRL	BAGLAN+	PR	3 C672	271	TOF; SCU5GG; 1.6 NS/M; 135 DEG;		
PB 206	RES PARAM	NDG			EA	LRL	BAGLAN+	NCSAC	33 106	D70				
PB 206	RES PARAM	TBL	83+6	10+7	1 +3	50+4	EJ	LRL	BOWMAN+	PR	178 1827	269		
PB 206	RES PARAM	NDG			EA	LRL	BOWMAN+	WASH	1127 96	469				
PB 206	RES PARAM	TBL	9 +6	10+7	7 +3	10+5	ED	LRL	BAGLAN	UCRL	50902	870		
PB 206	RES PARAM	TBL	9 +6	10+7	15+3	10+5	EJ	LRL	BAGLAN+	PR	3 C672	271		
PB 207	GN YIELD	GRPH	93+6		25+5	20+6	EJ	MIT	BERTOZZI+	PL	6 108	863	TOF; SC+H(NN); 50 DEG; TA TGT;	
PB 207	GN YIELD	GRPH	88+6	3 +3	25+4	EJ	LRL	BOWMAN+	PR	178 1827	269	TOF; SC+B10; 135 DEG;		
PB 207	GN DIF SIG	GRPH			25+4	35+5	EA	LRL	BOWMAN+	WASH	1136 78	969		
PB 207	GN DIF SIG	GRPH			20+4	15+6	EA	LRL	BOWMAN+	WASH	1136 83	969		
PB 207	GN DIF SIG	GRPH	84+6	98+6	15+4	10+6	ED	LRL	BAGLAN	UCRL	50902	870		
PB 207	GN DIF SIG	GRPH	84+6		15+4	30+5	EJ	LRL	BAGLAN+	PR	3 C672	271	TOF; SCU5GG; 1.1 NS/M; 135 DEG;	
PB 207	GN DIF SIG	GRPH	98+6		20+5	10+6	EJ	LRL	BAGLAN+	PR	3 C672	271	TOF; SC+H(NN); 0.6 NS/M; 135 DEG;	
PB 207	GN DIF SIG	GRPH	98+6		20+4	70+5	EJ	LRL	BAGLAN+	PR	3 C2475	671	TOF; SC+H(NN); 0.7 NS/M; 135 DEG;	
PB 207	RES PARAM	TBL	77+6	88+6	3 +3	25+4	EJ	LRL	BOWMAN+	PR	178 1827	269		
PB 207	RES PARAM	NDG			EA	LRL	BOWMAN+	WASH	1127 96	469				
PB 207	RES PARAM	TBL	74+6	98+6	14+4	57+5	ED	LRL	BAGLAN	UCRL	50902	870		
PB 207	RES PARAM	TBL	74+6	98+6	3 +3	98+5	EJ	LRL	BAGLAN+	PR	3 C672	271		
PB 207	STRNG FNC GO	TBL			EA	LRL	BAGLAN+	NCSAC	33 106	D70				
PB 207	STRNG FNC GO	TBL			EJ	LRL	BAGLAN+	PR	3 C672	271	$S(G0) = (13+/-7) \times 10^{-5}$			
PB 207	GN NON RESN	TEXT		40+4	EA	LRL	BOWMAN+	WASH	1136 78	969				
PB 207	GN NON RESN	NDG			EA	ANL		NCSAC	33 8	D70				
PB 207	DOORWAY STS	TEXT		20+5	70+5	EA	LRL	BOWMAN+	WASH	1136 83	969			
PB 207	DOORWAY STS	TEXT		20+5	60+5	ED	LRL	BAGLAN	UCRL	50902	870			
PB 207	DOORWAY STS	TEXT		50+4	20+5	ED	LRL	BAGLAN	UCRL	50902	870			
PB 207	DOORWAY STS	TEXT		20+5	55+5	EJ	LRL	BAGLAN+	PR	3 C2475	671	WGODS = 36.5 EV		
PB 207	DOORWAY STS	TEXT		50+4	20+5	EJ	LRL	BAGLAN+	PR	3 C2475	671	WGODS = 16.3 EV		
PB 207	DOORWAY STS	TEXT			EA	ANL	NELSON+	USNDC	1 15	572				
PB 208	GN YIELD	GRPH	93+6		25+5	20+6	EJ	MIT	BERTOZZI+	PL	6 108	863	TOF; SC+H(NN); 50 DEG; TA TGT;	
PB 208	GN YIELD	GRPH	93+6		25+5	20+6	EJ	MIT	BERTOZZI+	PL	6 108	863	TOF; SC+H(NN); 50 DEG; TA TGT;	
PB 208	GN YIELD	GRPH	9+6		3 +3	40+4	EJ	LRL	BOWMAN+	PR	178 1827	269	TOF; SC+B10; PULSE-SHAPE DISCRIM;	
PB 208	GN YIELD	GRPH	84+6		18+5	10+6	EA	ANL	TOOHEY+	NCSAC	42 24	N71	TOF; 90 AND 135 DEG;	
PB 208	GN YIELD	GRPH	84+6		18+5	95+5	EJ	ANL	TOOHEY+	PR	6 C1440	072	TOF; 90 AND 135 DEG;	
PB 208	GN ANG DISTR	NDG			EA	ANL	TOOHEY+	USNDC	1 13	572				
PB 208	GN DIF SIG	GRPH		1 +3	35+5	EA	LRL	BOWMAN+	WASH	1127 96	469			
PB 208	GN DIF SIG	GRPH	90+6		25+4	35+5	EJ	LRL	BOWMAN+	PRL	23 796	069	TOF; SCU5GG; 135 DEG;	
PB 208	GN DIF SIG	GRPH	98+6	10+7	5 +3	14+6	ED	LRL	BAGLAN	UCRL	50902	870		
PB 208	GN DIF SIG	GRPH	98+6		1 +3	35+5	EJ	LRL	BOWMAN+	PRL	25 1302	N70	TOF; SCU5GG; 135 DEG;	
PB 208	GN DIF SIG	GRPH	98+6		5 +3	33+5	EJ	LRL	BAGLAN+	PR	3 C672	271	TOF; SCU5GG; 1.0 NS/M; 135 DEG;	
PB 208	GN DIF SIG	GRPH	10+7		35+5	14+6	EJ	LRL	BAGLAN+	PR	3 C672	271	TOF; SC+H(NN); 0.8 NS/M; 135 DEG;	
PB 208	GN DIF SIG	GRPH	98+6		10+4	10+6	EJ	LRL	BAGLAN+	PR	3 C2475	671	TOF; SC+H(NN) AND SCU5GG; 135 DEG;	
PB 208	RES PARAM	TBL	93+6	10+7	26+5	85+5	EJ	MIT	BERTOZZI+	PL	6 108	863	WG FOR " RESONANCES"	
PB 208	RES PARAM	TBL	77+6	9 +6	3 +3	40+4	EJ	LRL	BOWMAN+	PR	178 1827	269		
PB 208	RES PARAM	NDG			EA	LRL	BOWMAN+	WASH	1827 96	469				
PB 208	RES PARAM	TBL	78+6	10+7	8 +3	86+5	ED	LRL	BAGLAN	UCRL	50902	870		

Nucleus Quantity	Type of data	E PRIM		E SEC		NT	LAB	Author(s)	Source	Year	Comments
		min	max	min	max						
PB 208 RES PARAM	TBL	98+6		30+4	86+5	EJ	LRL	BOWMAN+	PRL 25 1302	N70	
PB 208 RES PARAM	TBL	78+6	10+7	29+3	86+5	EJ	LRL	BAGLAN+	PR 3 C672	271	
PB 208 RES PARAM	TBL			18+5	95+5	EJ	ANL	TOOHEY+	PR 6 C1440	072	WGO AND JPI FOR 21 RESONANCES;
PB 208 STRNG FNC GO	TBL					EA	LRL	BAGLAN+	NCSAC 33 106	D70	
PB 208 STRNG FNC GO	TBL					EJ	LRL	BAGLAN+	PR 3 C672	271	S(G0)=(4.0+-3.6)E-5;
PB 208 GN NON RESN	NDG					EA	LRL	BOWMAN+	WASH 1127 96	469	
PB 208 GN NON RESN	TEXT	90+6		41+4		EJ	LRL	BOWMAN+	PRL 23 796	069	SIG(NR)=3.4 MB AT 40 KEV;
PB 208 GN NON RESN	TEXT			36+6	44+4	ED	LRL	BAGLAN	UCRL 50902	870	
PB 208 GN NON RESN	TEXT			41+4		TA	LRL	WEISS	NCSAC 31 102	570	
PB 208 GN NON RESN	TEXT			25+4	40+4	EA	ANL	JACKSON	NCSAC 33 8	D70	
PB 208 DOORWAY STS	TEXT	98+6		30+4	86+5	EJ	LRL	BOWMAN+	PRL 25 1302	N70	
PB 208 DOORWAY STS	TEXT	98+6		10+4	10+6	EJ	LRL	BAGLAN+	PR 3 C2475	671	7 M1 RESONANCES FROM 30 TO 860 KEV;
BI 209 GN YIELD	GRPH	83+6		1+3	10+6	EA	WRL	WINHOLD+	AERE PR/NP 16	869	
BI 209 GN DIF SIG	GRPH	11+7		1+3	13+4	EJ	LRL	BERMAN+	PRL 17 761	066	TOF; SC+B10; 15-30 NS/M; 135 DEG;
U 235 GN YIELD	NDG					EA	GA	SUND+	NCSAC 31 68	570	
U 235 GN YIELD	NDG					EA	ANL	JACKSON	NCSAC 33 12	D70	
U 238 GN YIELD	NDG					EA	GA	SUND+	NCSAC 31 68	570	
PU 239 GN YIELD	NDG					EA	GA	SUND+	NCSAC 31 68	570	
MANY RES PARAM	NDG					RC	ANL	BOLLINGER	66 WASH 2 1064 366		REV OF POSSIB-S THRSHLD MEASURMNTS;

MAIN REFERENCES

1. W.Bertozzi, C.P.Sargent, W.Turchinetz. Phys.Letters 6, 108, (1963).
2. L.M.Bollinger. Conf. on Neutron Cross Sections Technology. Washington, 1966. V.2, p.1064.
3. B.L.Berman, G.S.Sidhu, C.D.Bowman. Phys.Rev.Letters 17, 761 (1966).
4. C.D.Bowman, G.S.Sidhu, B.L.Berman. Phys.Rev. 163, 951 (1967).
5. B.L.Berman, R.L.VanHemert, C.D.Bowman. Phys.Rev. 163, 958 (1967).
6. R.L.VanHemert. UCRL-50501 (1968).
7. C.D.Bowman, B.L.Berman, H.E.Jackson. Phys.Rev. 178, 1827 (1969).
8. C.D.Bowman, B.L.Berman, R.J.Baglan. WASH-1127, 96 (1969).
9. E.J.Winhold et al. AERE-PR/NP-16, p. 33 (1969).
10. B.L.Berman, R.L.VanHemert, C.D.Bowman. Phys.Rev.Letters 23, 386 (1969).
11. C.D.Bowman, R.J.Baglan, B.L.Berman. WASH-1136, 78 (1969).
12. C.D.Bowman, R.J.Baglan, B.L.Berman. WASH-1136, 83 (1969).
13. B.L.Berman, S.C.Fultz, M.A.Kelly. WASH-1136, 87 (1969).
14. C.D.Bowman, R.G.Baglan, B.L.Berman. Phys.Rev.Letters 23, 796 (1969).
15. R.J.Baglan, C.D.Bowman, B.L.Berman. UCRL-72780 (1970).
16. B.L.Berman, R.J.Baglan, C.D.Bowman. Phys.Rev.Letters 24, 319 (1970).
17. H.E.Jackson. NCSAC-31, 10 (1970).
18. R.E.Sund et al. NCSAC-31, 68 (1970).
19. R.J.Baglan, C.D.Bowman. NCSAC-31, 100 (1970).
20. M.S.Weiss. NCSAC-31, 102 (1970).
21. R.J.Baglan. UCRL-50902 (1970).
22. C.D.Bowman et al. Phys.Rev.Letters 25, 1302 (1970).
23. NCSAC-33, 8 (1970).
24. H.E.Jackson. NCSAC-33, 9 (1970).
25. H.E.Jackson. NCSAC-33, 12 (1970).
26. R.J.Baglan, C.D.Bowman, B.L.Berman. NCSAC-33, 106 (1970).
27. R.J.Baglan, C.D.Bowman, B.L.Berman. Phys.Rev.C3, 672 (1971).
28. R.J.Baglan, C.D.Bowman, B.L.Berman. Phys.Rev. C3, 2475 (1971).
29. H.E.Jackson, E.N.Strait. Phys.Rev. C4, 1314 (1971).
30. ABRAMOV, A.I., KITAYEV, V.Ya., STAVISSKIJ, Yu.Ya., YUTKIN, M.G., in "Nejtronnaya Fizika", Pt. I, Naukova dumka, Kiev (1972).
31. H.E.Jackson, E.N.Strait. NCSAC-42, 23 (1971).
32. R.E.Toohey, H.E.Jackson. NCSAC-42, 24 (1971).
33. E.N.Strait, H.E.Jackson. NCSAC-42, 26 (1971).
34. H.E.Jackson, E.N.Strait. Phys.Rev.Letters 27, 1654 (1971).
35. B.H.Patrick, E.M.Bowey. AERE-PR/NP 18, 21 (1972).

36. H.E.Jackson, R.E.Toohey. USNDC 1, 13 (1972).
37. R.E.Toohey, H.E.Jackson. USNDC 1, 15 (1972).
38. K.L.Nelson, H.E.Jackson, R.E.Toohey. USNDC 1, 15 (1972).
39. K.H.Lokan et al. Phys.Rev.Letters 28, 1526 (1972).
40. H.E.Jackson, R.E.Toohey. Phys.Rev.Letters 29, 379 (1972).
41. R.E.Toohey, H.E.Jackson. Phys.Rev. C6, 1440 (1972).
42. E.J.Winhold et al. Phys.Letters 32B, 607 (1970).

SUPPLEMENTARY REFERENCES

- 1d. DZHELEPOV, D.S., PEKER, L.K., "Skhemy raspada radioaktivnykh yader ($A \leq 100$)", M.-L. "Nauka" (1966); DZHELEPOV, D.S., PEKER, L.K. SERGEEV, V.O., "Skhemy raspada radioaktivnykh yader ($A \geq 100$)" M.-L., USSR Academy of Sciences (1963).
- 2d. KRAVTSOV, B.A., "Massy atomov i energii svyazi yader, Moscow, Atomizdat (1965).
- 3d. J.H.Gibbons et al. Phys.Rev. 114, 1319 (1959).
- 4d. W.John, J.M.Prosser. Phys.Rev. 127, 231 (1962).
- 5d. M.N.Rao, J.Rapaport. Nuclear Data B3-5, 6-37 (1970).
- 6d. J.Rapaport. Nuclear Data, B3-5,6-85 (1970).
- 7d. R.L.Auble, J.Rapaport. Nuclear Data B3-3,4-1 (1970).
- 8d. M.N.Rao. Nuclear Data B3-3,4-43 (1970).
- 9d. H.W.Newson et al. Ann.Phys. (N.Y.) 8, 211 (1959).
- 10d. D.J.Hughes, R.B.Schwartz. BNL-325, 2nd Edition, 2nd Supplement. V.IIc (1966).
- 11d. C.D.Bowman, E.G.Bilpuch, H.W.Newson. Ann.Phys. 17, 319 (1962).
- 12d. R.G.Steiglitz. Ph.D.Thesis. RPI, 1970 (cm. [27]).
- 13d. J.A.Biggerstaff et al. Phys.Rev. 154, 1136 (1967).
- 14d. J.A.Farrell et al. Phys.Letters 17, 286 (1965).
- 15d. E.G.Bilpuch et al. Ann.Phys. 14, 387 (1961).
- 16d. R.W.Hockenbury et al. Phys.Rev. 178, 1746 (1969).
- 17d. N.B.Gove, A.H.Wapstra. Nuclear Data Tables 11, 127 (1972).
- 18d. ABRAMOV, A.I., Preprint FEI-337, Obninsk (1972).

C O N T E N T S

Foreword	1
Beryllium-9	5
Fluorine-19	6
Magnesium-24	7
Magnesium-25	9
Magnesium-26	11
Silicon-29	13
Phosphorus-31	15
Argon-40	16
Chromium-52	19
Chromium-53	21
Natural iron	26
Iron-56	29
Iron-57	31
Nickel-61	37
Tin-117	39
Tin-119	41
Natural lead	42
Lead-206	44
Lead-207	46
Lead-208	51
Bismuth-209	56
Annex 1. Some characteristics of stable and long-lived isotopes	57
Annex 2. Bibliographic index of work on photoneutron reactions near the threshold	71
Main references	75
Supplementary references	77